A shift resistant encoding in a rotor system

Marijn Waaijer

Technische Wiskunde en Natuurkunde
Bachelor thesis
TU Delft

Delft, September 4, 2019
Supervisors: J.M.A.M. Van Neerven,
B. M. Terhal

Contents

Introduction **2**

1 The rotor space **4**
1.1 The angular momentum operator 4
1.1.1 Shifts and Weyl relations 6
1.2 The angle operator on $l^2(\mathbb{Z})$ 6
1.3 Intermezzo: The problems related with number and phase 9
1.3.1 The original idea of the phase time operator 9
1.3.2 PVM's and POVM's 10
1.3.3 The time phase observable as POVM 12

2 Basic theory of quantum computing **16**
2.1 Quantum computing: The basics 16
2.2 Quantum Error Correction: Stabilizers 17
2.3 Quantum computation: Universality 18

3 Shift resistant codes **21**
3.1 The central idea of shift resistant quantum codes 21
3.2 Encoding in a quantum harmonic oscillator: The GKP code 24
3.3 Encoding in rotation-symmetric bosonic system 27

4 Quantum computation in a rotor system **31**
4.1 Encoding a qubit in a rotor 31
4.2 Quantum gates for the rotor space 35
4.2.1 The gate set for N = 1 35
4.2.2 The gate set for general N spacing 37

5 Physical realisation: superconducting qubits **40**
5.1 The Josephson junction 40
5.2 The transmon qubit 41
5.3 Two-Cooper-pair qubit 43

Conclusion **48**

Acknowledgments **49**

Introduction

A quantum computer is a computer which applies the properties described by quantum physics to process information. It is thought to be a very promising new technology of which the development forms one the main goals not only for Qutech at TU delft [1], but also for major computing companies such as IBM [2], Microsoft [3] and goole [4]. So the question arises: Why is quantum computing believed to be so promising? For this there are three main reasons [5]. The first reason is that there already exist algorithms which, by making use of the principles of quantum mechanics, are able to solve certain problems much faster than a classical computer can. The most famous example for this is the problem of finding the (unique) prime factorization of large integer numbers.[1] While a classical computer may take years (exponential time in the context of complexity theory) to crack this problem, an already developed algorithm, Shors algorithm, is thought to be able to solve the problem much faster (in polynomial time) [6]. The second reason is that for many other problems theoretical arguments for speedups exist, such as the simulation of quantum systems or optimization problems [7]. The last is that, and this argument somewhat implies the previous two, no classical computer can simulate a quantum computer, thus making it a truly new thing.

The arguments mentioned above paint a picture of why the quantum computer is new and can achieve things a classical computer never can. The next question then naturally follows: what can the quantum computer be used for? For some mathematical operations clear speedups, such as the before mentioned prime factorisation or for instance matrix inversion [5], are shown to be possible. In physics the quantum computer shows promise in the simulation of quantum systems, making it able to tackle unsolved problem in high energy physics and cosmology [8]. From a computer science perspective the quantum computer shows great potential for machine learning and the before mentioned optimization. Lastly the most important use for society is thought to be the simulation of large molecules, which used in the development of medicine and new materials [3].

Theoretically, following the description given above, any quantum system can principally be used to construct such a quantum computer. But of course not every quantum system forms a sensible candidate. One of the main questions in trying to build a quantum computer is thus, which quantum system to use to build it. To illustrate the relation between a quantum computer and the system it is built from, it is useful to look at the case of classical computing. A classical computer makes use of so called bits, which can be 0 or 1. Any two state system can be used to represent the 0 and 1, for instance orientation of a helix of a strand of DNA or two sides of a coin, but both of these systems are not very useful for computation. In classical computing the best way to represent the bits was found to be a high-low voltage distinction. In a classical computer the 1 bit represents a high voltage (a voltage higher than 2.2 Volt) and the 0 bit a low voltage (a voltage lower that 0.4 Volt). These voltages can be swiftly manipulated by a resistor, making the processing of information possible. Similarly, for the construction of a quantum computer a suitable two level system has to be chosen. In this report such a possible representing system is discussed.

So what makes this search for a suitable two level system so challenging? One of the reasons for this stems from a fundamental property of quantum mechanical systems - a quantum system cannot be measured without creating an uncontrollable disturbance in the system [5]. This has big implication for controlling the quantum bits, qubits, of the quantum computer. Since the state of

[1] This problem is so hard for a classical computer that it forms the basis of most encryption schemes for protecting data.

a quantum system can be disturbed by the environment, the state of the qubit can change from a 1 to a 0 state, causing an error in the calculation. The problem is now complicated by the fact that the state can not be simply checked by doing a measurement on the qubits, since this would disturb the calculation just as much as when it would be is going well. The problem is thus to not only find a two level system, but also design it in a way where the errors in the calculation can be detected and controlled.

The field of research interested in this question is called 'Quantum Error Correction' and it investigates, as the name implies, how to detect and correct errors (caused by the environment) in quantum computing. In Quantum Error Correction there are two ways to approach the previously mentioned problem. The first approach is to encode the information in more bits than originally necessary such that when a qubit obtains an error, the other qubits can be used to detect this error and obtain its original meaning. (This is somewhat similar to the technique used by CD's and DVD's to still play the right sound or film even if there are some scratches on them.) The second approach, and this is approach of this report, is to use error correction as one of the design foundations of the quantum computer.

The aim of this report is to theoretically study an example of such an intrinsically error-correcting design of the qubit. In the first three chapters some of the necessary theory for the theoretical description of these quantum computer designs is discussed. The design discussed here encodes the qubits in a rotor system. A rotor system is a system with rotational symmetry (and which keeps this symmetry over time). A mathematical study of the variables describing the rotor space, the angular momentum and angle of the position, and the relations between the two is provided in Chapter 1. Chapter 2 introduces most of the basic concepts used to describe the quantum computer. Special emphasis is placed on stabilizer measurements, which form the basis of the error correcting design, and on universality of a gate set, a gate being an operation on the qubit. Universality means every possible algorithm for the quantum computer can in principle be implemented. Chapter 3 uses the concepts of a stabilizer measurement to introduce the main concepts of an error correcting encoding design. The class of error correcting designs discussed here is called shift resistant encodings. After introducing the main concepts of shift resistant encodings, two examples are discussed. In Chapter 4 a theoretical shift resistant scheme of building a quantum computer in a rotor space is provided. The novelty presented here is that the encoding, which was constructed before in [9], is accompanied by a gate set which commutes with the small shift errors. This means that the gate set presented here, preserves the error correcting qualities of the encoded qubit. While this design is an interesting theoretical study, a possible realization is still far away. To study the current level of encoding qubits a realizable qubit design is discussed in Chapter 5. While this scheme is not fully shift resistant, it still uses many of the same error correcting principles in its design. The design expands on the concepts used to create the transmon qubit, which is one of the most successful qubits at this moment [10]. The main goal of the chapter is to study the Hamiltonian used to describe this new qubit design and learn what the eigenstates are. Lastly, in Chapter 6 a short conclusion and summary of the main results of this report are provided.

1. The rotor space

For the goal of encoding a qubit into a rotor system, it is important to have a full grasp of the mathematical details describing a rotor. A rotor represents a physical system with rotational symmetry, which, similar to the classical case, is best described using the angular momentum $\hat{L}$ and the angle $\hat{\Theta}$. It is in terms of the eigenstates of these operators that we will encode the qubit in chapter 4.

This Chapter is structured as follows. First the angular momentum operator is discussed along with the relevant Hilbert spaces associated with the description of the rotor, after which the shift operator and the floored angular momentum operator are introduced. After this the angle operator is discussed. First some pitfalls in the relation between the angular momentum operator and the angle operator are discussed, after which a construction of the angle operator is presented. This concludes the discussion of the rotor. In the last section of the chapter is an intermezzo in the discussion of encoding a qubit in a rotor. Here the related case of the number and time phase operator of an harmonic oscillator is discussed.

1.1 The angular momentum operator

The angular momentum operator is easiest defined on the Hilbert space of $l^2(\mathbb{Z})$. This is the Hilbert space of the two sided converging series a_l with $l \in \mathbb{Z}$ such that

$$l^2(\mathbb{Z}) = \{\underline{a} = (a_l)_{-\infty}^{\infty}, \sum_{l=-\infty}^{\infty} |a_l|^2 < \infty\}, \tag{1.1}$$

where the inner-product is defined as $(\underline{a}|\underline{b}) = \sum_{-\infty}^{\infty} a_l \overline{b_l}$ (which is always finite by the Cauchy-Schwartz inequality). Now for the series to represent a state we require that $\sum_{l=-\infty}^{\infty} |a_l|^2 = 1$.

Here the angular momentum state $|l\rangle$ is defined to be the series with a 1 on the l'th position and zeros everywhere else, meaning

$$|l\rangle = \begin{cases} a_n = 0, for\ n \neq l, \\ a_n = 1, for\ n = l. \end{cases} \tag{1.2}$$

The angular momentum operator is now defined to act on this state by

$$\hat{L}\,|l\rangle = l\,|l\rangle\,, l \in \mathbb{Z} \tag{1.3}$$

and this definition is extended by linearity. With this extension we should however be careful, because if we apply the operator on a series where $\sum_{l=-\infty}^{\infty} |la_l|^2$ diverges the result is not in $l^2(\mathbb{Z})$ any more and thus undefined. This means that the operator $\hat{L}$ is only well-defined on the domain of

$$\mathscr{D}(\hat{L}) = \left\{(a_l)_{l=-\infty}^{\infty} : \sum_{l=-\infty}^{\infty} |la_l|^2 < \infty\right\}. \tag{1.4}$$

With this choice of the domain, $\hat{L}$ can be shown to be self-adjoint. This completes the definition of the angular momentum operator.

Now we can use this definition to investigate the representation of the angular momentum operator on the Hilbert space of $L^2(0, 2\pi)$ with the normalized Lebesgue measure $\frac{d\theta}{2\pi}$ (and the

standard innerproduct of $(f|g) = \int_0^{2\pi} f\overline{g}\frac{d\theta}{2\pi}$). The Hilbert space of $l^2(\mathbb{Z})$ can be mapped to $L^2(0,2\pi)$ by the isometry given by the discrete Fourier transform of the series. This relation can be expressed as

$$\underline{a} = (...,a_{-1},a_0,a_1,a_2,...) \rightarrow \sum_{l=-\infty}^{\infty} a_l e^{il\theta} = f_a(\theta) \tag{1.5}$$

and this relation expresses an isometry since

$$\sum_{l=-\infty}^{\infty} |a_l|^2 = \frac{1}{2\pi}\int_0^{2\pi} |f_a(\theta)|^2 d\theta. \tag{1.6}$$

To see how the angular momentum operator acts on $L^2(0,2\pi)$ we take the discrete Fourier transform of equation 1.3. By following the transformation of equation 1.5 we can see that the state $|l\rangle$ is represented by $e^{il\theta}$ in $L^2(0,2\pi)$. This gives that the angular momentum should act, in its representation on $L^2(0,2\pi)$, as

$$\hat{L}e^{il\theta} = le^{il\theta}, \tag{1.7}$$

from which we can conclude that the angular momentum operator is given on $L^2(0,2\pi)$ by

$$\hat{L} = -i\frac{\partial}{\partial\theta}, \tag{1.8}$$

which is defined on the domain of

$$\mathscr{D}(\hat{L}) = \{f \in L^2(0,2\pi) : f' \in L^2(0,2\pi)\}. \tag{1.9}$$

This domain is equivalent to the domain of equation 1.4 by using the Fourier transform.

The 'floored' angular momentum operators

In order to achieve a error resistant encoding we make use of angular momentum operators with a floored eigenspectrum. These 'floored' angular momentum operators (for any $k \in \mathbb{N}$) are defined to act on the eigenstates of $\hat{L}$ as

$$\left\lfloor \frac{\hat{L}}{k} \right\rfloor |l\rangle = \left\lfloor \frac{l}{k} \right\rfloor |l\rangle, l \in \mathbb{Z}, k \in \mathbb{N}, \tag{1.10}$$

and this definition is extended by linearity on the domain of the operator. Maybe somewhat surprisingly, the domain of $\lfloor \frac{\hat{L}}{k} \rfloor$ given by

$$\mathscr{D}(\hat{L}) = \left\{ (a_l)_{l=-\infty}^{\infty} : \sum_{l=-\infty}^{\infty} |\left\lfloor \frac{l}{k} \right\rfloor a_l|^2 < \infty \right\} \tag{1.11}$$

is the same as that of the 'unfloored' version of $\hat{L}$. This means that we (mathematically) do not loose any of the states allowed by $\hat{L}$ by adding the floored angular momentum operators to our arsenal of possible operators.

Here we will shortly prove this claim of $\mathscr{D}(\hat{L}) = \mathscr{D}(\lfloor \frac{\hat{L}}{k} \rfloor)$ for a fixed $k \in \mathbb{N}$. Firstly the case of $\mathscr{D}(\hat{L}) \subseteq \mathscr{D}(\lfloor \frac{\hat{L}}{k} \rfloor)$ is somewhat trivial. Since the eigenvalues of the flooring function, in absolute value, are always smaller than the regular angular momentum, we obtain that $\sum_{l=-\infty}^{\infty} |\lfloor \frac{l}{k} \rfloor a_l|^2 \leqslant \sum_{l=-\infty}^{\infty} |la_l|^2 < \infty$. Therefore $\mathscr{D}(\hat{L}) \subseteq \mathscr{D}(\lfloor \frac{\hat{L}}{k} \rfloor)$. Secondly we prove the sightly harder case of $\mathscr{D}(\lfloor \frac{\hat{L}}{k} \rfloor) \subseteq \mathscr{D}(\hat{L})$, let $(a_l)_{l=-\infty}^{\infty} \in \mathscr{D}(\lfloor \frac{\hat{L}}{k} \rfloor)$. Then, since $\sum_{l=-\infty}^{\infty} |\lfloor \frac{l}{k} \rfloor a_l|^2 < \infty$ and $|\lfloor \frac{l}{k} \rfloor| \leqslant |\lfloor \frac{l}{k} \rfloor|^2$, it also holds that $\sum_{l=-\infty}^{\infty} |(\lfloor \frac{l}{k} \rfloor \pm 1)|a_l|^2 < \infty$. From this we can also conclude that $k\sum_{l=-\infty}^{\infty} |(\lfloor \frac{l}{k} \rfloor \pm 1)|^2 |a_l|^2 < \infty$, leading to the final result of $\sum_{l=-\infty}^{\infty} |(k\lfloor \frac{l}{k} \rfloor + sign(l)k)|^2 |a_l|^2 < \infty$. Now we remark that $|k\lfloor \frac{l}{k} \rfloor + sign(l)k| \geqslant |l|$ for all $l \in \mathbb{Z}$. Thus by the same argument as above we conclude that $\mathscr{D}(\lfloor \frac{\hat{L}}{k} \rfloor) \subseteq \mathscr{D}(\hat{L})$. Thereby we obtain the claimed result of $\mathscr{D}(\hat{L}) = \mathscr{D}(\lfloor \frac{\hat{L}}{k} \rfloor)$.

Here we also note that the operator defined above can be shown to be self-adjoint, where the prove is basically the same as the (unfloored) angular momentum operator $\hat{L}$. We thereby conclude the floored angular momentum operators to be legitimate quantum mechanical observables on the domain $\mathscr{D}(\hat{L})$.

1.1.1 Shifts and Weyl relations

For the encoding of the qubit in a rotor setting some state operations need to be defined. The main state operations on the rotor space are given by the state shift operator $\hat{V}$ and the phase shift operator $e^{i\alpha\hat{L}}$. In this section both operators are introduced and their commutation relation are shown.

The state and phase shift operator

For the angular momentum eigenstates the state shift operator $\hat{V}$ can be defined as

$$\hat{V}\left|l\right\rangle = \left|l+1\right\rangle. \tag{1.12}$$

and can be extended by linearity as

$$\hat{V}(...,a_{-2},a_{-1},a_0,a_1,a_2...) = (...,a_{-3},a_{-2},a_{-1},a_0,a_1,...). \tag{1.13}$$

Note that this operator retains the norm, $\sum_{n\in\mathbb{Z}}|a_n|^2 = \sum_{n\in\mathbb{Z}}|a_{n-1}|^2$, and acts surjectively on the Hilbert space. This makes the state shift operator a unitary operator.

Since $\hat{L}$ and $\left\lfloor\frac{\hat{L}}{k}\right\rfloor$ are self adjoint they generate groups of unitary operators of the form $e^{i\alpha\left\lfloor\frac{\hat{L}}{k}\right\rfloor}$, with $\alpha\in\mathbb{R}$. Note that for $k=1$, the floored operator is simply the regular angular momentum operator. These unitary operators act on the eigenstates as

$$e^{i\alpha\left\lfloor\frac{\hat{L}}{k}\right\rfloor}\left|l\right\rangle = e^{i\alpha\left\lfloor\frac{l}{k}\right\rfloor}\left|l\right\rangle, \alpha\in\mathbb{R}. \tag{1.14}$$

Because of this action these operators are called the phase shift operators.

The Weyl commutation relations

The commutation of the phase and the state shift operator is given by Weyl relations. These Weyl relations are given by

$$e^{i\alpha\left\lfloor\frac{\hat{L}}{k}\right\rfloor}(\hat{V}^k)^m = e^{i\alpha m}(\hat{V}^k)^m e^{i\alpha\left\lfloor\frac{\hat{L}}{k}\right\rfloor},\ k\in\mathbb{N},\ m\in\mathbb{Z}, \tag{1.15}$$

which is an expression very often used in calculating the error propagation. Here we want to prove these Weyl relations.

This is easily done by applying both sides of the equation to the eigenstates. This gives that

$$\begin{aligned} e^{i\alpha\left\lfloor\frac{\hat{L}}{k}\right\rfloor}(\hat{V}^k)^m\left|l\right\rangle &= e^{i\alpha\left\lfloor\frac{\hat{L}}{k}\right\rfloor}\left|l+km\right\rangle \\ &= e^{i\alpha\left\lfloor\frac{l+km}{k}\right\rfloor}\left|l+km\right\rangle = e^{i\alpha(\left\lfloor\frac{l}{k}\right\rfloor+m)}\left|l+km\right\rangle \\ &= e^{i\alpha m}e^{i\alpha\left\lfloor\frac{l}{k}\right\rfloor}\left|l+km\right\rangle \text{ and} \end{aligned} \tag{1.16a}$$

$$\begin{aligned} e^{i\alpha m}(\hat{V}^k)^m e^{i\alpha\left\lfloor\frac{\hat{L}}{k}\right\rfloor}\left|l\right\rangle &= e^{i\alpha m}(\hat{V}^k)^m e^{i\alpha\left\lfloor\frac{l}{k}\right\rfloor}\left|l\right\rangle = e^{i\alpha m}e^{i\alpha\left\lfloor\frac{l}{k}\right\rfloor}(\hat{V}^k)^m\left|l\right\rangle \\ &= e^{i\alpha m}e^{i\alpha\left\lfloor\frac{l}{k}\right\rfloor}\left|l+km\right\rangle, \end{aligned} \tag{1.16b}$$

which proves equation 1.15.

1.2 The angle operator on $l^2(\mathbb{Z})$

The second observable, conjugate to the angular momentum operator, used to describe the rotor is the angle operator $\hat{\Theta}$. This operator represents the angle of the position of the particle with respect to the rotation axis. Most intuitively this operator is represented on the Hilbert space of $L^2(0,2\pi)$, where it simply acts as a multiplication given by $\hat{\Theta}f(\theta) = \theta f(\theta)$. But since the conserved states are easily expressed by the angular momentum states, we want to find an expression of the angle operator which acts in the $l^2(\mathbb{Z})$ Hilbert space of the angular momentum.

However this proves to be not an easy task, as is shown in the paragraph below. There we show that a naïve construction of the angle operator by demanding $[\hat{L}, \hat{\Theta}] = i$ will never work. Instead their commutation needs to act on the Weyl level as presented above. These commutation relations provide a candidate operator. We then show this operator to act as desired and explain why the commutation relation of $[\hat{L}, \hat{\Theta}] = i$ fails.

The pitfall of a naïve construction of the angle operator

The construction of the angle operator has some subtle problems. Since angular momentum and angle mirror momentum and position, the naïve desire would be to construct a angle operator on $l^2(\mathbb{Z})$ satisfying the commutation relation

$$[\hat{L}, \hat{\Theta}] = i. \tag{1.17}$$

However, this proves to be a dead end.

The reason for this is given by the application of the commutation to the $|l\rangle$ eigenstates. This gives

$$\langle l' | [\hat{L}, \hat{\Theta}] | l \rangle = i \langle l' | l \rangle = i\delta_{l'l}, \tag{1.18}$$

while at the same time, by the self-adjointness of $\hat{L}$ (which gives $\langle l' | \hat{L} = l' \bar{l'}$), we get

$$\langle l' | [\hat{L}, \hat{\Theta}] | l \rangle = \langle l' | \hat{L}\hat{\Theta} | l \rangle - \langle l' | \hat{\Theta}\hat{L} | l \rangle = (l' - l) \langle l' | \hat{\Theta} | l \rangle, \tag{1.19}$$

which gives i = 0 if l' = l, which is clearly wrong. (see also [11]). This shows that a more carefull approach for the construction of the angle operator is required.

The construction of the angle operator

As noted before, because of the analogy with position and momentum, the angular momentum and angle operator are expected to commute up to a phase. Only this commutation does not happen on the 'operator level' but instead on the set of unitary operators they generate. This commutation is given by the Weyl relations. In this case of the angle and angular momentum this relation is desired to take the form of

$$e^{i\alpha\hat{L}} e^{ik\hat{\Theta}} = e^{ik\alpha} e^{ik\hat{\Theta}} e^{i\alpha\hat{L}}. \tag{1.20}$$

The goal here is to construct a $\hat{\Theta}$ operator which satisfies this relation (see also [12]).

For this goal the shift operator reveals its value. The unitary shift is a unitary operator, which satisfies the required relation of

$$e^{i\alpha\hat{L}} \hat{V}^k = e^{ik\alpha} \hat{V}^k e^{i\alpha\hat{L}}. \tag{1.21}$$

By the spectral theorem for normal (or unitary) operators [13], there must now be a self-adjoint operator (conveniently named) $\hat{\Theta}$ such that $\hat{V}^k = e^{ik\hat{\Theta}}$ for $k \in \mathbb{Z}$.

In order to show that this conveniently named operator actually is the angular position operator, we first off start with the definition of the angular position operator. The angular position operator is defined to act as

$$\hat{\Theta}|\theta) = \theta|\theta). \tag{1.22}$$

These 'eigenstates' are actually improper eigenstates (improper because they are non-normalizable), which is why they are not denoted by a regular ket symbol. They are given by[1]

$$|\theta) = \sum_{l \in \mathbb{Z}} e^{-il\theta} |l\rangle. \tag{1.23}$$

It is somewhat to be expected that the eigenstates of the angular position are improper, since the angular position can take any value between 0 and 2π, which is an uncountable set, but is here only represented by countably many numbers.

[1] The following manipulations can be made mathematically rigorous by the notion of approximative eigenvalues.

From this definition we can further define the before mentioned $e^{ik\hat{\Theta}}$. For this we remark that from the definition of equation 1.22 it follows that for $n \in \mathbb{N}$ we get,

$$\hat{\Theta}^n|\theta) = \theta^n|\theta), \tag{1.24}$$

with which we can define $e^{i\hat{\Theta}}$ by

$$e^{i\hat{\Theta}} = \sum_{n=0}^{\infty} \frac{i\hat{\Theta^n}}{n!}. \tag{1.25}$$

This operator acts on the eigenstates in an expected manner as

$$e^{i\hat{\Theta}}|\theta) = \sum_{n=0}^{\infty} \frac{i\hat{\theta^n}}{n!}|\theta) = e^{i\theta}|\theta). \tag{1.26}$$

Now in order to see the claimed relation between the operator $e^{i\hat{\Theta}}$ and the shift operator from above, we let the shift operator act on the eigenstates. Because the states do not converge, the action of $\hat{V}$ on the eigenstate is not properly defined, but can be understood by taking truncated sums (for large M)

$$\hat{V} \sum_{l=-M}^{M} e^{-il\theta}\,|l\rangle = \sum_{l=-M}^{M} e^{-il\theta}\,|l+1\rangle = \sum_{l=-M+1}^{M+1} e^{-i(l-1)\theta}\,|l\rangle = e^{i\theta} \sum_{l=-M+1}^{M+1} e^{-il\theta}\,|l\rangle\,. \tag{1.27}$$

This gives that

$$\hat{V}|\theta) = e^{i\theta}|\theta) = e^{i\hat{\Theta}}|\theta), \theta \in [0, 2\pi), \tag{1.28}$$

showing the claimed relation of $\hat{V}^k = e^{ik\hat{\Theta}}$ to hold.

To gain a more explicit form of angular position $\hat{\Theta}$ operator, we again make use of the spectral theorem. Since we know the spectrum of $\hat{\Theta}$ to be $[0, 2\pi]$ the operator can be represented as

$$\hat{\Theta} = \int_0^{2\pi} \theta|\theta)(\theta|\frac{d\theta}{2\pi}, \tag{1.29}$$

where the mathematically rigorous interpretation of the integral is as a spectral integral, with $|\theta)(\theta|\frac{d\theta}{2\pi}$ as the spectral measure. Using this form of the operator, we can rewrite this to

$$\begin{aligned}
\int_0^{2\pi} \theta|\theta)(\theta|\frac{d\theta}{2\pi} &= \int_0^{2\pi} \theta(\sum_{m\in\mathbb{Z}} e^{-im\theta}\,|m\rangle)(\sum_{n\in\mathbb{Z}} e^{-in\theta}\,\langle n|)\frac{d\theta}{2\pi} \\
&= \frac{1}{2\pi}\int_0^{2\pi} \theta \sum_{m,n\in\mathbb{Z}} e^{i(n-m)\theta}\,|m\rangle\langle n|\,d\theta \\
&= \frac{1}{2\pi}\sum_{m,n\in\mathbb{Z}} \int_0^{2\pi} \theta e^{i(n-m)\theta} d\theta\,|m\rangle\langle n| \\
&= \frac{1}{2\pi}\sum_{m\neq n} \Bigg([\theta \frac{1}{i(n-m)} e^{i(n-m)\theta}]_0^{2\pi} \\
&\quad - \int_0^{2\pi} \frac{1}{i(n-m)} e^{i(n-m)\theta} d\theta) \Bigg)\,|m\rangle\langle n| - \frac{1}{2\pi}\sum_{n\in\mathbb{Z}} \int_0^{2\pi} \theta d\theta\,|n\rangle\langle n| \\
&= \sum_{m\neq n} \frac{1}{i(n-m)}\,|m\rangle\langle n| - \pi\hat{I},
\end{aligned} \tag{1.30}$$

which results in

$$\hat{\Theta} = \sum_{m\neq n} \frac{1}{i(n-m)}\,|m\rangle\langle n| - \pi\hat{I}. \tag{1.31}$$

This gives the required explicit form of the angular position operator.

Why $[\hat{L}, \hat{\Theta}] = i$ fails

So why does the naïve construction of the $\hat{\Theta}$ by $[\hat{L}, \hat{\Theta}] = i$ fail then? For this we have to look at the domain of $\hat{\Theta}$ (simply defined by $\{\underline{a} \in l^2 : \hat{\Theta}\underline{a} \in l^2(\mathbb{Z})\}$). If $\hat{\Theta}$ acts on the eigenstates $|l\rangle$ on $l^2(\mathbb{Z})$ we obtain

$$\hat{\Theta}\,|l\rangle = \pi\,|l\rangle + \sum_{m \neq l} \frac{1}{i(l-m)}\,|m\rangle\,. \tag{1.32}$$

This state is still in the $l^2(\mathbb{Z})$ Hilbert space, but lies outside of the domain of $\hat{L}$ given by equation 1.4. Thus we conclude that the image of $\hat{\Theta}$ acting on the eigenstates $|l\rangle$ and the domain of $\hat{L}$ are disjoint, making the expression $\langle l'|\,\hat{L}\hat{\Theta}\,|l\rangle$ non-sense, which leads to the contradictions from above (meaning those from 1.19).

This means that although the standard indicator of two observables being conjugate, the commutation relation $[\hat{L}, \hat{\Theta}] = i$, fails, the angle operator as an observable conjugate to the angular momentum can still be constructed.

1.3 Intermezzo: The problems related with number and phase

As a short intermezzo in the discussion of the rotor space, we here to take a look at the related case of the number $\hat{n}$ and time phase operator $\hat{\phi}$. This time phase operator $\hat{\phi}$ was for a while thought to be the conjugate observable of the number operator $\hat{n}$, in somewhat analogous sense to the relation between the angular momentum and angular position from above. The key difference however is that in this case the associated Hilbert spaces are $l^2(\mathbb{N})$ and $L^2(0, 2\pi)$. This difference between $l^2(\mathbb{N})$ and $l^2(\mathbb{Z})$ leads to the fact that the construction of a time phase operator, as a variable conjugate to the number operator, as a 'standard' quantum mechanical observable was shown to not be possible [14]. But still this phase operator is used in the literature, as for example in [15] (which will be discussed further in Chapter 3). In this section first the problems with the construction of the phase operator as a 'standard' quantum mechanical observable is discussed, after which some of the possible solutions, as are used in [15], are discussed.

1.3.1 The original idea of the phase time operator

The original idea of constructing a phase operator came from the well-known solution the differential equation of a classical harmonic oscillator, given by

$$X = Re^{i\phi} + R^* e^{-i\phi}, \tag{1.33}$$

with R the amplitude and ϕ the phase. The goal became to construct an operator which could represent a measurement of this ϕ for the quantum mechanical harmonic oscillator. Mirroring the classical result above is the quantum mechanical position operator $\hat{Q}$ written in terms of the raising operator $\hat{a}^+$ and the lowering operator $\hat{a}^-$, given as

$$\hat{Q} = \hat{a}^+ + \hat{a}^-. \tag{1.34}$$

This let to the idea of trying to decompose the raising operator as

$$\hat{a}^+ = \hat{R}e^{i\hat{\phi}}, \tag{1.35}$$

where $\hat{R}$ was named the amplitude operator and $\hat{\phi}$ the time phase operator. The form of the amplitude operator is easily derived to be

$$\hat{R}^2 = \hat{R}e^{i\hat{\phi}}e^{-i\hat{\phi}}\hat{R} = \hat{a}^+\hat{a}^- = \hat{n}. \tag{1.36}$$

Thus goal became to decompose the raising operator as

$$\hat{a}^+ = \sqrt{\hat{n}}e^{i\hat{\phi}}. \tag{1.37}$$

This relation results in the commutation relation of

$$[\hat{n}, \hat{a}^+] = \hat{a}^+ \implies [\hat{n}, e^{i\hat{\phi}}] = e^{i\hat{\phi}} \implies [\hat{n}, \hat{\phi}] = i, \tag{1.38}$$

where in the last step the supposed unitarity of $e^{i\hat{\phi}}$ is used. This gave rise to the idea of a time phase $\hat{\phi}$ operator conjugate to the number operator $\hat{n}$ [14].

The problems with these wishes

As mentioned in the introduction, the construction of a time phase operator $\hat{\phi}$ which satisfies the requirements from above does not exist. As a first note, the commutation of equation 1.38 has problems similar to equations 1.18 and 1.19, being

$$\left\langle n' \right| \left[\hat{n}, \hat{\phi}\right] \left| n \right\rangle = i \left\langle n' | n \right\rangle = i\delta_{n'n}, \tag{1.39a}$$

$$\left\langle n' \right| \left[\hat{n}, \hat{\phi}\right] \left| l \right\rangle = \left\langle n' \right| \hat{n}\hat{\phi} \left| n \right\rangle - \left\langle n' \right| \hat{\phi}\hat{n} \left| n \right\rangle = (n' - n) \left\langle n' \right| \hat{\phi} \left| n \right\rangle, \tag{1.39b}$$

which again leads to $i = 0$ for $n' = n$. This show direct construction from 1.38 to be impossible.

The second and more prominent of the problems can be seen by the effect of the lowering operator on a number state $|n\rangle \in l^2(\mathbb{N})$, which is given by $\hat{a}^- |n\rangle = \sqrt{n} |n-1\rangle$ for $n \geqslant 1$. From this it is concluded that (again for $n \geqslant 1$)

$$\hat{a}^- |n\rangle = e^{-i\hat{\phi}} \sqrt{\hat{n}} |n\rangle = \sqrt{n} |n-1\rangle \implies e^{-i\hat{\phi}} |n\rangle = |n-1\rangle. \tag{1.40}$$

Thus we see that $e^{-i\hat{\phi}}$ is desired to act as left shift operator on $l^2(\mathbb{N})$. In similar manner we can derive that $e^{i\hat{\phi}}$ is desired to act as the right shift operator, again on $l^2(\mathbb{N})$.

The problem with these shift operators on $l^2(\mathbb{N})$ is that they are not unitary (as opposed to the shift operator $\hat{V}$ from above). That these operators are not unitary can be seen by taking a state $\Psi \in l^2(\mathbb{N})$, with $\Psi = (a_1, a_2, a_3, ..)$, $a_1 \neq 0$, and letting the right shift operator defined as $V_r(a_1, a_2, a_3, ...) = (0, a_1, a_2, ...)$ (which is the supposed role of $e^{i\hat{\phi}}$) and the left shift operator defined as $V_l(a_1, a_2, a_3, ...) = (a_2, a_3, a_4...)$ (which is the supposed role of $e^{-i\hat{\phi}}$) act in succession on this state. This gives

$$V_r V_l \Psi = (a_2, a_3, ..) = (0, a_2, a_3, ..) \neq (a_1, a_2, a_3, ..) = \Psi, \tag{1.41}$$

from which we conclude that $e^{i\hat{\phi}} e^{-i\hat{\phi}} \neq \hat{I}$. Thus we conclude that $e^{i\hat{\phi}}$ is not unitary, from which directly follows that there is no self-adjoint operator satisfying the decomposition of equation 1.35 (for more see [14] and [11]).

1.3.2 PVM's and POVM's

So how do we still say something about the time phase of a system, as is being done in [15]? The solution is to use instead of the 'standard' quantum mechanical observable, which is represented by a Projection Valued measure (PVM), a so-called (normalized) Positive Operator Valued Measure or POVM. A POVM is used to describe an open system, meaning for example a system in which the experimenter plays a role or a system which is a mixture of states, as opposed to a closed system for which PVMs are used. The solution of formulating the time phase in terms of POVM is a limited solution. While a 'perfect' phase observable can not be constructed, the description of some measurements are possible with this POVM. Only in this limited sense of POVMs that can we say something about the time phase of a system.

Here we first introduce the idea of a projection valued measure, which is the measure behind the 'standard' quantum mechanics as described in for instance [16]. Understanding the measure of 'standard' quantum mechanics we can introduce the concept of a POVM. With an understanding of this concept of a POVM some of the phase POVMs can be discussed in the next section.

The projection-valued measure

A projection valued (PV) measure is defined (from [13]) as follows.

Definition 1 (Projection Valued measure)**.** *A projection valued measure on a metric space M is a mapping $P : \mathscr{B}(M) \to \mathscr{L}(H)$ that assigns to every Borel subset $B \subseteq M$ an orthogonal projection (operator) $P_B := P(B) \in \mathscr{L}(H)$ with the following properties:*

1. $P_M = I$

2. *for all* $x \in H$ *the mapping* $B \to \langle x, P_B x\rangle = P_x(B)$ *, with* $B \in \mathscr{B}(M)$*, defines a measure on* M*.*

To place this definition in the context of quantum mechanics, we remark that in quantum mechanics only norm 1 vectors are used, making the measure above a probability measure (by condition 1 of theorem above, see [17]). To see how this acts as probability measure, note that we calculate the probability of obtaining $|\Psi\rangle$ as a measurement outcome of a system in state $|\xi\rangle$ is given by use of the projection operator of $|\Psi\rangle$ as $\langle\xi|\,|\Psi\rangle\langle\Psi|\,|\xi\rangle = |\langle\xi|\Psi\rangle|^2$, with $0 \leqslant |\langle\xi|\Psi\rangle|^2 \leqslant 1$.

In the context of quantum mechanics as a probability theory, self-adjoint operators, which are used to represent observables, assume the role of the expectation value. This can be seen by the following theorem from [18], for which we first have to define self-adjointness for unbounded operators (from [13]) as this will be an important distinction with POVMs later.

Definition 2 (self-adjoint operator)**.** *A densely defined operator* $\hat{A}$ *on a Hilbert space* H *is called self-adjoint if* $D(A) = D(A^*)$ *and* $\hat{A}h = \hat{A}^*h$ *for all* h *in this common domain, where* $\hat{A}^*$ *is the adjoint operator of* $\hat{A}$*.*

Theorem 1 (Spectral theorem for self-adjoint operators)**.** *Let a* $\hat{A}$ *be a self-adjoint operator on* H*, then there exists a unique projection-valued measure* P *on* $\sigma(T)$ *such that*

$$\hat{A} = \int_{\sigma(T)} \lambda dP(\lambda) \tag{1.42}$$

with $\sigma(T)$ *the spectrum of* T *and* $\lambda \in \sigma(T)$*.*

Where the spectrum is the set of $\lambda \in \mathbb{C}$ such that $\hat{A} - \lambda\hat{I}$ is not invertible. The spectrum is a concept closely related to eigenvalues and, as is the case for eigenvalues, for a self-adjoint operator the spectrum is always real. Thus by this theorem we see that an observable is represented as a self-adjoint operator, which can be decomposed as a 'weighted sum' of the projection operators weighted by the spectrum of A (as in $\int_{\sigma(T)} \lambda dP(\lambda)$).

To conclude: in 'standard' quantum quantum mechanics the probability of finding a state $|\Psi\rangle$ as measurement outcome when measuring a system in state $|\xi\rangle$is done by using the projection operator $P_{|\Psi\rangle}$ on the inner-product as $\left\langle \xi \middle| P_{|\Psi\rangle}\xi \right\rangle$, which forms a probability measure. In this case expectation values of observable can be represented by self-adjoint operators by use of the spectral theorem.

Positive Operator Valued (POV) measures

In the paragraph above we saw how 'standard' quantum mechanics functions as a probability theory. Here we do the same, but then we expand the setting to allow for mixtures of states. First we shortly recap this way of doing quantum mechanics. After that the measure used for this is presented and the paragraph is concluded with some characterizations of the observable in this context.

The state of a system ρ is represented here as a an operator with trace 1, where the trace is calculated for some finite dimensional Hilbert space as $tr[\rho] = \sum_i^N \langle\phi_i|\rho\phi_i\rangle$, where ϕ_i is an orthonormal basis. This trace does not depend on which orthonormal basis ϕ_i is used to calculate the trace. This concept can then be broadened to the infinite dimensional case for all trace class operators. An operator is trace class if the sum $\sum_i^\infty \langle\phi_i||\rho|\phi_i\rangle$ converges for the operator $|\rho| = (\rho^*\rho)^{\frac{1}{2}}$ [13].

The measure behind this way of doing quantum mechanics is the already mentioned positive operator valued measure. This measure is defined the following [12]

Definition 3 (Normalized Positive Operator Valued measure)**.** *A normalized positive operator valued measure on a metric space* M *is a mapping* $E : \mathscr{B}(M) \to \mathscr{L}(H)$ *that assigns to every Borel subset* $B \subseteq M$ *an operator* $E(B)$ *with the following properties:*

1. $E(X) \geqslant 0$ *for all* $X \in \mathscr{B}(M)$ *(Where an operator* $\hat{A} \geqslant 0$*, if* $\left\langle \phi \middle| \hat{A}\phi \right\rangle \geqslant 0$ *for all* $\phi \in H$*)*

2. $E(M) = I$

3. $E(\cup X_i) = \sum E(X_i)$ *for all disjoint sequences* $(X_i) \subseteq M$

This measure becomes a probability measure by use of the following theorem (based on [12]). For this let $\mathscr{T}(H)$ be the set of trace class operators and let $S(H)$ be the set of positive trace one operators (thus the set of possible states), as

$$S(H) = \{T \in \mathscr{T}(H) | T \geqslant 0, tr[T] = 1\}, \tag{1.43}$$

then

Theorem 2. *For any POV measure* $E : \mathscr{B}(M) \to \mathscr{L}(H)$ *and any* $T \in S(H)$ *the mapping*

$$p_T^E : \mathscr{B}(M) \to [0,1], X \to p_T^E(X) = tr[TE(X)] \tag{1.44}$$

is a probability measure.

Here we can interpret the number $0 \leqslant p_T^E(X) \leqslant 1$ as the probability that a measurement of the observable E performed on the state T leads to a result in the set of measurement outcomes X.

So how can we think of these observable representing operators E? Where in the setting of PV-measures observables were represented by self-adjoint operators, they are here represented by symmetric operators, which are defined as follows

Definition 4. *A densely defined operator* $\hat{A}$ *on a Hilbert space* H *is called symmetric if* $\left\langle \hat{A}h \middle| h \right\rangle = \left\langle h \middle| \hat{A}h \right\rangle$ *for all* $h \in \mathscr{D}(A)$.

Do note that we here only require that $\mathscr{D}(\hat{A}) \subseteq \mathscr{D}(\hat{A}^*)$, which is of-course a weaker requirement than $\mathscr{D}(\hat{A}) = \mathscr{D}(\hat{A}^*)$ (as was required for self-adjoint operators). Thus we can see that a broader class of observables is allowed here. We also see by this weaker requirement that every PV measure is a POV measure, but not vice versa. For this symmetric operator we then calculate the expectation value of a measurement of $\hat{A}$ on the state ρ by $\langle \hat{A} \rangle = Tr[\hat{A}\rho]$.

A second important result on these POV measures is a result somewhat mirroring the spectral theorem voor unitary operators. Where the spectral theorem relates unitary operators and self-adjoint operators (and thus to PV measures), this theorem relates contractions, meaning an operator $\hat{C}$ such that $||\hat{C}h|| \leqslant ||h||$ for all $h \in H$, to POV measures.

Theorem 3. *For every contraction* $\hat{C}$ *acting on a Hilbert space there exists exactly one POV measure* F *such that*

$$\hat{C}^n = \int_0^{2\pi} e^{inx} dF(x) \tag{1.45}$$

for n = 0, 1, 2, ... If C is unitary then F is a PV measure.

With this broader context of contractions and POVMs an observable for the time phase can be constructed.

Again as a short recap: in the setting where aside from just PVM also POVM are used to calculate the probabilities of quantum mechanical experiments, the state is represented by a positive trace-1 operator. The probability of finding a measurement outcome in the set X is then given by $tr[TE(X)]$, where $E(X)$ is the POVM associated to the measured observable, which are represented by the broader class of symmetric operators. Lastly, for each contraction a unique POVM can be constructed associated to this contraction.

1.3.3 The time phase observable as POVM

Here we use the theory of POVMs to construct a possible representation of measurement of the time phase, as used in [15]. With this POVM we also construct a phase 'observable'. This 'observable' does commute according to equation 1.38 on a dense domain, but is still limited in its use. This section is based on [12].

We start again from the right $\hat{V}_r$ and left $\hat{V}_l$ shift operators from above and note here that although these operators are not unitary, they are both contractions. Using the result from above we obtain that there exists a unique POV such that

$$\hat{V}_l^n = \int_0^{2\pi} e^{in\phi} dM(\phi). \tag{1.46}$$

This somewhat mirrors the use of Stone's theorem in the relation $\hat{V}^k = e^{ik\hat{\Theta}}$ from the angular momentum case.

Somewhat mirroring the Weyl relation (equation 1.20) is the relation between the left shift and the phase shift $e^{i\phi\hat{n}}$ associated to the number operator $\hat{n}$, given by

$$e^{i\phi\hat{n}}\hat{V}_l e^{-i\phi\hat{n}} = e^{i\phi}\hat{V}_l. \tag{1.47}$$

This relation holds on all eigenstate $|n\rangle$, $n \geqslant 1$, but becomes somewhat trivial for $|0\rangle$ as both sides will simply become the zero-function. By using $V = \int_0^{2\pi} e^{i\phi} dM(x)$ (from equation 1.46 for the case of $n = 1$), this does result in

$$e^{i\phi'\hat{n}} \int_0^{2\pi} e^{i\phi} dM(\phi) e^{-i\phi'\hat{n}} = \int_0^{2\pi} e^{i\phi} (e^{i\phi'\hat{n}} dM(\phi) e^{-i\phi'\hat{n}}) = \int_0^{2\pi} e^{i(\phi-\phi')} dM(\phi), \tag{1.48}$$

where we see that

$$(e^{i\phi'\hat{n}} dM(\phi) e^{-i\phi'\hat{n}}) = dM(\phi - \phi'). \tag{1.49}$$

Because then by substituting $u = \phi - \phi'$ we get

$$\int_0^{2\pi} e^{i\phi} dM(\phi + \phi') = \int_0^{2\pi} e^{i(u-\phi')} dM(u). \tag{1.50}$$

This shows that the $e^{i\phi'\hat{n}}$ will in fact shift the phase, in the same way the $e^{i\alpha\hat{L}} |\theta\rangle = |\theta - \alpha\rangle$.

With this result we can go on to try to construct the measure $dM(\phi)$ in a more explicit form. Consider the Hilbert space $L^2(0, 2\pi)$, again with the normalized lebesgue measure $\frac{d\phi}{2\pi}$, and the basis $|\xi_k\rangle = e^{ik\phi}$ with $k \in \mathbb{Z}$. Then the space of $l^2(\mathbb{N})$ can be mapped to $L^2(0, 2\pi)$ by the (isometric) map

$$W : l^2(\mathbb{N}) \to L^2(0, 2\pi), W : \Psi \to \sum_{k=0}^{\infty} e^{ik\phi} \langle n|\Psi\rangle, \tag{1.51}$$

which forms a Fourier series with only the positive terms. Here we interpreted $W(\Psi)$ as the representation of the state in the phase-space of $L^2(0, 2\pi)$. Now we can define the probability of finding the phase in the set $X \in B(0, 2\pi)$, denoted by $M(X)$, for any $\eta, \psi \in l^2(\mathbb{N})$ by representing them in the phase-space of $L^2(0, 2\pi)$ and using the indication function 1_X. This procedure gives

$$\begin{aligned}
\langle \eta|M(X)\psi\rangle &:= \int_0^{2\pi} 1_X \overline{W(\eta)} W\psi \frac{d\phi}{2\pi} \\
&= \int_X \Big(\sum_{n=0}^{\infty} e^{-in\phi} \langle \eta|n\rangle \Big) \Big(\sum_{m=0}^{\infty} e^{im\phi} \langle m|\Psi\rangle \Big) \frac{d\phi}{2\pi} \\
&= \frac{1}{2\pi} \sum_{n,m=0}^{\infty} \int_X e^{-in\phi} e^{im\phi} d\phi \langle \eta|n\rangle\langle m|\Psi\rangle \\
&= \frac{1}{2\pi} \sum_{n,m=0}^{\infty} \int_X e^{i(m-n)\phi} d\phi \langle \eta|n\rangle\langle m|\Psi\rangle,
\end{aligned} \tag{1.52}$$

where the sums and integral can be swapped due to the monotone convergence theorem [17]. Thus we conclude that

$$M(X) = \frac{1}{2\pi} \sum_{n,m=0}^{\infty} \int_X e^{i(m-n)\phi} d\phi \, |n\rangle\langle m|, \tag{1.53}$$

which is the POVM representation of a phase measurement as for instance used in [15].

With this POVM we can also construct a (somewhat limited) phase operator $\widehat{\phi_{M^1}}$, by taking the first moment of the measure from above. This gives that

$$\begin{aligned}
\widehat{\phi_{M^1}} &:= \int_0^{2\pi} \phi M(d\phi) \\
&= \frac{1}{2\pi} \sum_{n,m=0}^{\infty} \int_0^{2\pi} \phi e^{i(m-n)\pi} d\phi \, |n\rangle\langle m| \\
&= \frac{1}{2\pi} \sum_{n=0}^{\infty} \int_0^{2\pi} \phi d\phi \, |n\rangle\langle n| + \frac{1}{2\pi} \sum_{n\neq m}^{\infty} \int_0^{2\pi} \phi e^{i(m-n)\phi} d\phi \, |n\rangle\langle m| \\
&= \frac{1}{2\pi} 2\pi^2 \, |n\rangle\langle n| + \frac{1}{2\pi} \sum_{n\neq m}^{\infty} \left([\frac{1}{i(m-n)} \phi e^{i(m-n)\phi}]_0^{2\pi} - \int_0^{2\pi} \frac{1}{i(m-n)} e^{i(m-n)\pi} d\phi \right) |n\rangle\langle m| \\
&= \pi \, |n\rangle\langle n| + \frac{1}{2\pi} \sum_{n\neq m}^{\infty} \frac{1}{i(m-n)} 2\pi e^{i(m-n)2\pi} \, |n\rangle\langle m| \\
&= \pi \hat{I} - i \sum_{n\neq m}^{\infty} \frac{1}{(m-n)} \, |n\rangle\langle m| \, .
\end{aligned} \tag{1.54}$$

This operator has been presented as a candidate operator for the 'phase operator' in [19].

In a very similar manner we can derive the second moment operator of the measure $M(X)$. This gives [12]

$$\begin{aligned}
\widehat{\phi_{M^2}} &:= \int_0^{2\pi} \phi^2 M(d\phi) \\
&= ... = \frac{3}{4}\pi^2 + \sum_{m\neq n} \left(\frac{2\pi i}{(n-m)} + \frac{2}{(n-m)^2} \right) |n\rangle\langle m| \, .
\end{aligned} \tag{1.55}$$

The derivation is omitted here due its length and similarity to the case from above. But more importantly, we remark that for this operator it holds that

$$\begin{aligned}
(\widehat{\phi_{M^1}})^2 = \left(\pi \hat{I} - i \sum_{n\neq m}^{\infty} \frac{1}{(m-n)} \, |n\rangle\langle m| \right)^2 \neq \\
\frac{3}{4}\pi^2 + \sum_{m\neq n} \left(\frac{2\pi i}{(n-m)} + \frac{2}{(n-m)^2} \right) |n\rangle\langle m| = \widehat{\phi_{M^2}},
\end{aligned} \tag{1.56}$$

as can clearly be seen from the prefactor of the identity operator. This shows how this 'phase observable' is limited by being a POVM.

The big virtue of this operator however is that $\widehat{\phi_{M^1}}$ actually satisfies the commutation relation of

$$[\hat{n}, \widehat{\phi_{M^1}}]\Psi = -i\Psi \tag{1.57}$$

on the domain of

$$\mathscr{D}_{commutation} = \{\Psi \in l^2(\mathbb{N}) | \sum_{n=0}^{\infty} n|a_n|^2 < \infty, \sum_{n=0}^{\infty} a_n = 0\} \tag{1.58}$$

which is dense in the domain of $\hat{n}$, given by $\mathscr{D}(\hat{n}) = \{\Psi = (a_1, a_2, ...) \in l^2(\mathbb{N}) | \sum_{n=1}^{\infty} n|a_n|^2 \leqslant \infty\}$, as is proven in [19]. Note that $|n\rangle \notin \mathscr{D}_{commutation}$, which shows that the result of equation 1.39 is not properly defined. For the proof of the relation 1.57, let $|\Psi\rangle = \sum_{k=0}^{\infty} a_k \, |k\rangle \in \mathscr{D}_{commutation}$,

then

$$
\begin{aligned}
[\hat{n}, \widehat{\phi_{M^1}}]\,|\Psi\rangle &= \hat{n}\widehat{\phi_{M^1}}\,|\Psi\rangle - \widehat{\phi_{M^1}}\hat{n}\,|\Psi\rangle \\
&= \hat{n}\left(\pi\hat{I} - i\sum_{n\neq m}^{\infty}\frac{1}{(m-n)}\,|n\rangle\langle m|\right)|\Psi\rangle - \left(\pi\hat{I} - i\sum_{n\neq m}^{\infty}\frac{1}{(m-n)}\,|n\rangle\langle m|\right)\hat{n}\,|\Psi\rangle \\
&= \hat{n}\pi\hat{I}\,|\Psi\rangle - \pi\hat{I}\hat{n}\,|\Psi\rangle - \hat{n}\left(i\sum_{n\neq m}^{\infty}\frac{1}{(m-n)}\,|n\rangle\langle m|\right)|\Psi\rangle + \left(i\sum_{n\neq m}^{\infty}\frac{1}{(m-n)}\,|n\rangle\langle m|\right)\hat{n}\,|\Psi\rangle \\
&= -\hat{n}\left(i\sum_{n\neq m}^{\infty}\frac{1}{(m-n)}\,|n\rangle\langle m|\right)\sum_{k=0}^{\infty}a_k\,|k\rangle + \left(i\sum_{n\neq m}^{\infty}\frac{1}{(m-n)}\,|n\rangle\langle m|\right)\hat{n}\sum_{k=0}^{\infty}a_k\,|k\rangle \\
&= -\hat{n}\left(i\sum_{n\neq m}^{\infty}\frac{1}{(m-n)}\,|n\rangle\sum_{k=0}^{\infty}a_k\langle m|k\rangle\right) + \left(i\sum_{n\neq m}^{\infty}\frac{1}{(m-n)}\,|n\rangle\langle m|\right)\sum_{k=0}^{\infty}ka_k\,|k\rangle \\
&= -\hat{n}\left(i\sum_{n\neq m}^{\infty}\frac{1}{(m-n)}a_m\,|n\rangle\right) + \left(i\sum_{n\neq m}^{\infty}\frac{1}{(m-n)}\,|n\rangle\sum_{k=0}^{\infty}ka_k\langle m|k\rangle\right) \\
&= -\left(i\sum_{n\neq m}^{\infty}\frac{a_m n}{(m-n)}\,|n\rangle\right) + \left(i\sum_{n\neq m}^{\infty}\frac{ma_m}{(m-n)}\,|n\rangle\right) \\
&= -i\sum_{n\neq m}^{\infty}\frac{(n-m)a_m}{(m-n)}\,|n\rangle \\
&= i\sum_{n\neq m}^{\infty}a_m\,|n\rangle = i\sum_{n=0}^{\infty}\left(\sum_{m\neq n}^{\infty}a_m\right)|n\rangle = -i\sum_{n=0}^{\infty}a_n\,|n\rangle = -i\,|\Psi\rangle\,,
\end{aligned}
\tag{1.59}
$$

where in the last step it was used that $\sum_{n=0}^{\infty}a_n = 0 \Leftrightarrow \sum_{n\neq m}^{\infty}a_n = -a_m + \sum_{n=0}^{\infty}a_n = -a_m$. We do remark here however that this commutation does not extend to a commutation on the Weyl level (as was the case with the angular position operator) [19].

This phase operator from equation 1.54 does however have some limited use. Firstly, since a POV measure was used the moments are not the operator applied multiple times, meaning $(\widehat{\phi_{M^1}})^l \neq \int_0^{2\pi}\phi^l M(d\phi)$ for $l \geqslant 2, l \in \mathbb{Z}$, as was shown for the case of $l = 2$. Secondly, it carries a non-uniqueness, by freedom in the choice of the origin, due to the shifts of equation 1.49. (For more on this, see [12].) Therefore the POVM is mostly used for phase measurement with M(X) and not for the determination of the expectation of the phase with $\widehat{\phi_{M^1}}$, as could be seen for instance in [15].

The idea of a phase operator started with the decomposition of the raising operator as $\hat{a}^+ = \sqrt{\hat{n}}e^{i\hat{\phi}}$, where $\hat{\phi}$ was thought to be the time phase operator of an harmonic oscillator. From the properties of the raising operator we concluded that the $e^{i\hat{\phi}}$ operator should act as the right shift operator on $l^2(\mathbb{N})$. Since this operator is not unitary, no self-adjoint operator $\hat{\phi}$ could be constructed (analogous to the method used for the angular momentum operator). But since the right shift operator was a contraction, we shifted from using the standard projection valued (PV) measure to using a positive operator valued (POV) measure. This positive operator valued measure made it possible to perform phase measurements, as are used in [15]. By taking the first moment of this POVM a phase observable was constructed which did commute with the $\hat{n}$ on the Heisenberg level, but was limited by its use to determine higher moments and its non-uniqueness.

This derivation show that although $\hat{L}$ and $\hat{n}$ act very similar, the difference in the Hilbert between $l^2(\mathbb{Z})$ and $l^2(\mathbb{N})$ has large consequence for the construction of their conjugate variable. Where in the former case the resulting operator can be represented in the standard form as a PV measure, for the latter the POV measures had to be introduced to still make measurements possible.

2. Basic theory of quantum computing

In order to implement quantum computing in a rotor setting and to understand the advantage of doing so some basic concepts from the theory on quantum computing need to be introduced. The first is the introduction of stabilizers from the theory of quantum error correction. The setting is the following: Due to the environment the state of the qubits can alter, causing errors in the computation. In order to achieve stable and reliable quantum computation these errors need to be detected and corrected. The goal of the field of quantum error correction is to do this detection and correction in the most efficient way possible, without destroying the superposition of the computationally relevant states a (logical) measurement. A short introduction presenting some crucial results from this field, namely the use of stabilizers, will form the first part of this chapter.

The second introduction is in the theory on complete gate sets. All computers, be it classical or quantum, have two basic components: bits and gates. The bits hold the information used in the computation and the gates alter the state of the bits. By reading out the alteration of the qubits the result of the calculation can be concluded. By sequencing the operations of different gates, new operations can be achieved. The main focus of the part of the chapter will be to find the minimal number of gates necessary to perform every unitary bit operation. Here such a complete gate set is presented and it consists (amazingly) of only 4 gates.

2.1 Quantum computing: The basics

In order to reach the goals stated above, some general concepts about the theoretical setting of quantum computing need to be introduced first.

The qubit

The most basic component of the quantum computer is a qubit. The qubit represented on the Hilbert space of $\mathbb{C}^2$ by vector with norm 1. For the computation with qubit 2 orthonormal bases $|0\rangle, |1\rangle$ and $|+\rangle, |-\rangle$ are most commonly used. $|0\rangle$ and $|1\rangle$ are commonly denoted by

$$|0\rangle = \begin{bmatrix} 1 \\ 0 \end{bmatrix}, \ |1\rangle = \begin{bmatrix} 0 \\ 1 \end{bmatrix}. \tag{2.1}$$

For these bases the following relations hold

$$|+\rangle = \frac{1}{\sqrt{2}}(|0\rangle + |1\rangle), \ |-\rangle = \frac{1}{\sqrt{2}}(|0\rangle - |1\rangle). \tag{2.2}$$

As noted in the introduction, the qubit is used as a representation of an underlying physical state in the language of computer science.

Since the total quantum state is invariant under global phase shifts (meaning $\left\langle e^{i\phi}\Psi\right| A \left|e^{i\phi}\Psi\right\rangle$ is the same for all $\phi \in [0, 2\pi]$), the qubit can be represented on a sphere called the Bloch sphere. For a graphical representation see figure 2.1 below. This Bloch sphere is mainly used to track the effects of bit operations. Bit operations are represented by unitary matrices, which, due to their unitarity, can be represented by a rotation of this Bloch sphere.

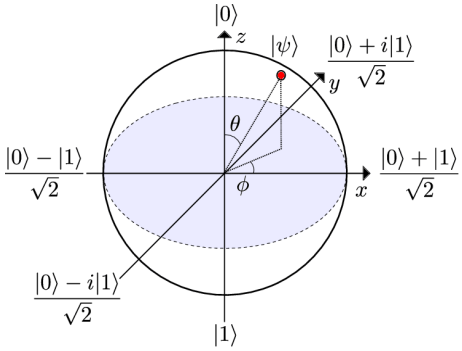

Figure 2.1: The Bloch sphere

The Pauli group

The most basic operations on the Bloch sphere are the rotations around the x-, y- and z- axes. These operations are given by the Pauli operators, a name taken from the Pauli spin operators and form a group generated by two elements. These generating operators are the bit-flip operator$\hat{X}$, with eigenbasis $\{|+\rangle, |-\rangle\}$, and the phase-flip operator Z, with eigenbasis $\{|0\rangle, |1\rangle\}$. The operators $\hat{X}$ and$\hat{Z}$are represented in the basis form equation 2.1 by

$$\hat{X} = \begin{bmatrix} 0 & 1 \\ 1 & 0 \end{bmatrix}, hatZ = \begin{bmatrix} 1 & 0 \\ 0 & -1 \end{bmatrix}. \tag{2.3}$$

The Pauli group for 1 qubit is then given by

$$P_1 = \{\pm\hat{I}, \pm i\hat{I}, \pm\hat{X}, \pm iX, \pm\hat{Y}, \pm i\hat{Y}, \pm hatZ, \pm ihatZ\} = \langle\hat{X}, iI, \hat{Z}\rangle. \tag{2.4}$$

For more qubits the generators are the generators of the single qubit case acting on each qubit separately. So 1 qubit generator $\langle\hat{X}\rangle$ for 2 qubits would be replaced by $\langle\hat{X}\otimes I, I\otimes\hat{X}\rangle$.

2.2 Quantum Error Correction: Stabilizers

As mentioned in the introduction the difficult thing about quantum error corrections is that an error has to be detected without disturbing superpositions by a measurement. The solution to this problem is provided by stabilizer measurements. Here a basic introduction into the theory of stabilizers is provided.

Stabilizers

The goal of a quantum error correcting scheme is to be able to check whether the qubit is in the desired state without disturbing the state if it actually is. This means that a measurement S is required with the following property

$$\hat{S}\,|\Psi\rangle_{desired} = |\Psi\rangle_{desired}\,. \tag{2.5}$$

This measurement S is called a stabilizer of $|\Psi\rangle$. Clearly the identity operator always fits this requirement. But if S is not the identity operator, then there exist $|\psi\rangle \neq |\psi\rangle_{required}$ such that will give $S\,|\psi\rangle_1 = c\,|\psi\rangle_2$. This means that a non-1 measurement will signal that the state is not in the desired state. Meaning that an error has been detected. But if there is no error, the state stays in the desired state. So a stabilizer measurement acts as the identity on the required state, but differs for other states.

An example of a stabilizer measurement is given by the Pauli $\hat{Z}$ operator on $|0\rangle$. Letting $\hat{Z}$ work on $|0\rangle$, we get $\hat{Z}\,|0\rangle = |0\rangle$, thus $\hat{Z}$ acts as an identity here. But letting $\hat{Z}$ work on $|1\rangle$ gives $\hat{Z}\,|1\rangle = -\,|1\rangle$, so if the state collapses under a $\hat{Z}$ measurement to $|1\rangle$ this can be detected as a non $+1$-measurement. As a consequence if the desired state is $|0\rangle$ any deviation in the

superposition can be detected, since for $|\Psi\rangle = \alpha|0\rangle + \beta|1\rangle$ with $\alpha, \beta \in \mathbb{C}, |\alpha|^2 + |\beta|^2 = 1, |\alpha|^2 \neq 1$ we get $Z|\Psi\rangle = \alpha|0\rangle - \beta|1\rangle \neq |\Psi\rangle$. This means that $\hat{Z}$ can be used to detect any change in the superposition, but fails to detect any change in the phase (since $\hat{Z}|\Psi\rangle = |\Psi\rangle$ for any $|\alpha|^2 = 1$).

The theory on stabilizer measurement can be split up in two parts, one part where the stabilizer measurements S are fixed and the other part where the state $|\Psi\rangle$ is fixed. First the effect of fixing the stabilizer S is discussed. Here it is noted that if two linearly independent vectors $|\psi\rangle_1, |\psi\rangle_2$ are stabilized by the measurement S, then a linear combination is also stabilized by S. (Since $S(a|\psi_1\rangle + b|\psi_2\rangle) = aS|\psi_1\rangle + bS|\psi_2\rangle = a|\psi_1\rangle + b|\psi_2\rangle$). So for every stabilizer operator S, there is an associated linear subspace V_S which contains all the states stabilized by S. Using the previous example we saw that $V_Z = \{|\Psi\rangle = \alpha|0\rangle, \alpha \in \mathbb{C}, |\alpha|^2 = 1, \}$.

This has two important consequences. First by combining two stabilizer measurement $S_1 \neq S_2$, by applying them for instance as $S_1 S_2|\psi\rangle$, the intersection of the two subspaces can be stabilized. In formal terms: let $V_{S_1} \cap V_{S_2} \neq \varnothing$, then for any $|\Psi\rangle \in V_{S_1} \cap V_{S_2}$ it holds that $S_1 S_2|\psi\rangle = |\psi\rangle$. Secondly if an operator C commutes with the stabilizer S, then applying C will not move the state out of the subspace fixed by S. Moreover if C commutes with all the elements from a set of stabilizers M_s, C will again not move the state out of the stabilized subspace. In conclusion any unitary operator S with at least one degenerate eigenvalue $\lambda = 1$ can be used to fix an associated linear subspace V_S on which any commuting operator can act without moving the states out of the subspace.

Secondly the effect of fixing the state $|\Psi\rangle$ is discussed. Here it is noted that the norm-1 vectors $|\Psi\rangle \in N_1 = \{|\Psi\rangle \in \mathbb{C}^2, ||\Psi\rangle|^2 = 1\}$ and the bit operations by the group of unitary matrices $\mathbf{U} = \{U \in GL(2,\mathbb{C}), U \textit{ unitary}\}$ form a group action (see [20] for more on group actions). Now for a fixed $|\Psi\rangle \in N_1$ the stabilizer of $|\Psi\rangle$ in $\mathbf{U}$ is defined as

$$S_{|\Psi\rangle} = \{U \in \mathbf{U} : U|\Psi\rangle = |\Psi\rangle\}. \tag{2.6}$$

There are two important results from group theory in this definition. The first is that is that the stabilizer set as defined above forms a subgroup in the larger group of $\mathbf{U}$ for any $|\Psi\rangle \in N_1$. Since the intersection of two subgroups always forms a subgroup, it becomes meaningful to talk about a group of stabilizer $\mathrm{S} = \cap_{i=1}^{n} S_{|\Psi\rangle_i}$. The second result is that for $|\Psi\rangle_2 = U|\Psi\rangle_1$ with $U \in \mathbf{U}$ it holds that $S_{|\Psi\rangle_2} = U S_{|\Psi\rangle_1} U^{-1} = \{USU^{-1}, S \in S_{|\Psi\rangle_1}\}$, making it easy to calculate the need stabilizers after a bit operation.

In conclusion, a group of stabilizers can be used to detect when the state moves out the linear subspace associated to the group of stabilizers. Any operator commuting with all the individual stabilizers will keep the state in this associated linear subspace and can thus be used 'freely' on the subspace.

2.3 Quantum computation: Universality

As presented above the Pauli operators play a central role in quantum computation, this central role is emphasized further here. The role of the Pauli subgroup in the group of all unitary operators is crucial in achieving universal quantum computation. Universality, in this context, means that every possible bit operation, represented by a unitary operator, should be possible to implement on the quantum computer. Here a very surprising fact is discovered: every unitary operator U can be approximated by V (also unitary), under the norm $E(U,V) = max_{|\psi\rangle}(||(U-V)|\psi\rangle||)$, where V is in a set generated by only four unitary operators (or gates). Meaning that only four gates are required to achieve this universality under approximation. This set is given by the following theorem [21]:

Theorem 4 (universality)**.** *The Clifford group together with any other gate not in the Clifford group form a universal set of quantum gates.*

The Clifford group

The Clifford group C_n is the normalizer group of the Pauli group P_n in the group of unitary operators. This means that $C_n = \{U \text{ unitary and } \forall p_1 \in P_n, \exists p_2 \in P_n : U p_1 U^\dagger = p_2\}$. As has

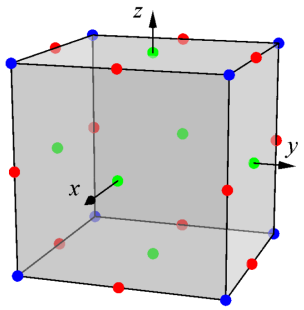

Figure 2.2: The group actions of the Clifford group on the Bloch sphere are denoted by the rotational symmetries of a cube. The different colours of the dots denote the different types rotational axes of the rotational symmetries.

been noted above, any unitary transformation can be seen as a rotation on the Bloch sphere. The Clifford group acting on a single qubit corresponds in this picture to the rotation symmetries of a (3d) cube (see figure 2.2). This can be used to prove that by adding a non-Clifford gate this gates set provides universality for a single qubit. All the possible computations done by only using the Clifford group can be easily simulated on a classical computer. This is shown by the following theorem:

Theorem 5 (Gottesman - Knill theorem)**.** *Any quantum computation involving only:*

1. *state preparation in the computational basis*
2. *Clifford group operations*
3. *measurements in the standard basis*
4. *any classical control conditioned on the measurement outcomes*

can be perfectly simulated in polynomial time on a probabilistic classical computer.

Thus the addition of a gate which is not in the Clifford group actually "promotes" the computer to the quantum level.

The Clifford group forms again a finite group and is generated by only three of its elements. These generating gates are the Hadamard gate H, the Phase gate P and the controlled-ROT ($\hat{C}_{rot}$) gate. Thus the Clifford group is represented by $\langle \hat{H}, \hat{S}, \hat{C}_{rot} \rangle$. The Hadamard gate and the Phase gate are single qubit operations and thus are best represented by a matrix. The matrices, using the basis given by 2.1, are given by:

$$\hat{H} = \frac{1}{2}\begin{bmatrix} 1 & 1 \\ 1 & -1 \end{bmatrix}, \ \hat{S} = \begin{bmatrix} 1 & 0 \\ 0 & i \end{bmatrix} \tag{2.7}$$

The $\hat{C}_{rot}$ gate acts on two qubits: a control bit and a target bit. The operation of the $\hat{C}_{rot}$ gate is best described in the following way. If the control bit is $|0\rangle$, then it does nothing. If the control bit is $|1\rangle$, then it applies the phase-flip operator $\hat{Z}$ on the target bit. Important to note here is that $\hat{C}_{rot}$ gate does not measure the state of the control bit, but can act on a superposition states.

The extra element: the T-gate

Theorem 4 gives us that once the Clifford group is obtained only one non-Clifford has to be added. Since the Clifford group is finite and the group of unitary gates is uncountable, there is a plethora of options. Here we presented only one option, namely the T-gate. The gate acts as the square root of the phase gate, meaning $\hat{T}^2 = \hat{S}$. The matrix representation of the T-gate is given by

$$\hat{T} = \begin{bmatrix} 1 & 0 \\ 0 & e^{i\frac{\pi}{4}} \end{bmatrix}. \tag{2.8}$$

In the rotor encoding presented in chapter 4, the T-gate will form the non-Clifford element to complete the universal gate set.

To conclude: by describing how the Clifford gates and the T-gate gate can be constructed, a universal quantum computer can be build.

3. Shift resistant codes

One of the main questions when building a quantum computer is what physical system to use to represent the quantum bits. In classical computing a high-low voltage difference is used to represent the 0 and 1 bit states. What the most effective physical system to represent (to encode) these bits for quantum computing is, as was mentioned in the introduction, is still an open question. A first idea was to use a simple two level quantum system, such as for example electron spin [22] or the polarization of photons [23]. In this case however the challenge of building a quantum computer is to make the bits as stable as possible, but any actual measuring and correcting of potential errors has to be done by encoding the information into multiple bits. This naturally gives rise to the question whether an encoding is possible, where the detection and correction of errors is part of the qubit design itself.

This can, at least theoretically, be done in the form of shift resistant codes. These encodings take a large superposition of states with a high degree of symmetry as its physical system to represent its qubit, as opposed to a single spin state. This symmetry results in invariance under certain operations, which is then used to detect small errors in the encoding by measuring asymmetries. This idea forms the fundamental motivation of building a quantum computer in a rotor space, or any shift resistant encoding. The inspiration of encoding a qubit into a rotor space comes from important previous work, where a qubit was encoded in the position and momentum of quantum harmonic oscillator and the number of bosons. In this chapter both of the previous methods are presented in order to show their relation to the encoding in the rotor setting.

3.1 The central idea of shift resistant quantum codes

As stated in the introduction, the most crucial step is to take a superposition of states with some symmetry to represent a qubit, in order to allow for the detection and correction of small errors in the encoding itself. This idea is best understood in a smaller toy model and then expanded to the larger, more realistic scenarios, such as a harmonic oscillator. (Courtesy of [24].)

The toy model

The smaller toy model consists of an 18 dimensional system. The possible states are given by $|j\rangle$, with $j \in \{1, 2, ..17, 18\}$. On these states two operators, $\hat{S}$ (shift) and $\hat{P}$ (phase), act as

$$\hat{S}\,|j\rangle = |j + 1 \; mod \; 18\rangle \tag{3.1a}$$

$$\hat{P}\,|j\rangle = \omega^j\,|j\rangle\,, \omega = e^{\frac{i2\pi}{18}} \tag{3.1b}$$

The goal is to encode states which are resistant to errors of the following type: $\hat{S}^a\hat{P}^b$ with $a, b \in \{-1, 0, 1\}$. Here $\hat{S}^0$, $\hat{P}^0$ are defined to be the identity operator.

For this purpose the qubit could be represented as

$$|\bar{0}\rangle = \frac{1}{\sqrt{3}}(|0\rangle + |6\rangle + |12\rangle), \tag{3.2a}$$

$$|\bar{1}\rangle = \frac{1}{\sqrt{3}}(|3\rangle + |9\rangle + |15\rangle). \tag{3.2b}$$

The stabilizer of the qubits

These states could then be stabilized by $\hat{S}^6, \hat{P}^6$. This combination of states and stabilizer protects the qubit from the small shifts mentioned above. To show this first it is proven that the qubit is actually stabilized by $\hat{S}^6, \hat{P}^6$, after which it is shown how error are detected using these stabilizers.

Here we shortly prove that the states given by equation 3.2 are stabilized by $\hat{S}^6, \hat{P}^6$, meaning that the qubit states from above are a $+1$-eigenvalue states of $\hat{S}^6, \hat{P}^6$. First we note that all the states differ by 6, thus $\hat{S}^6 |\bar{0}\rangle = |\bar{0}\rangle$ and $\hat{S}^6 |\bar{1}\rangle = |\bar{1}\rangle$. Also note that the states numbers $k = |k\rangle$ all form multiples of 3, so 18 is a divisor of 6k for any non-zero k, resulting in the fact that $w^{6k} = 1$. So these states are invariant under applying the operator $\hat{P}^6$. (Note that $\hat{P}$ acts as an identity on the $|0\rangle$ state.) Showing the claimed $\hat{S}^6, \hat{P}^6$ to be stabilizers.

Now in order to detect the errors of the form $\hat{S}^a \hat{P}^b$ with $a, b \in \{-1, 0, 1\}$, the following commutation relations are used

$$(\hat{S}^a \hat{P}^b)\hat{S}^6 = \omega^{6b} \hat{S}^b (\hat{S}^a \hat{P}^b) \tag{3.3a}$$

$$(\hat{S}^a \hat{P}^b)\hat{P}^6 = \omega^{6a} \hat{P}^b (\hat{S}^a \hat{P}^b). \tag{3.3b}$$

Since for the errors 6b or 6a will never form a multiple of 18, this gives that $\omega^{6a}, \omega^{6b} \neq 1$. Therefore we can detect whether an error has occurred. Now since we have only allowed errors of the type $\hat{S}^a \hat{P}^b$ with $a, b \in \{-1, 0, 1\}$, we can not only detect the error, but also identify which error has occurred and correct it by applying the inverse of the error. This makes the encoding fully protected against these errors. The case of errors other than the type mentioned above will be discussed later on.

Relations between the errors

The encoding protects the bits from small errors in both the "main dimension", meaning state alterations by operator $\hat{S}$, and the Fourier transformed domain, meaning phase shifts by operator $\hat{P}$. This Fourier relation between the two error types holds for all shift resistant encodings. As for instance in a harmonic oscillators, where both errors in position $|q\rangle$ as in its Fourier transformed domain the momentum $|p\rangle$ are likely to happen.

As a consequence of this Fourier relation, more protection against one type of error means less protection against the other. By spacing out the $|j\rangle$ states more, the encoding can be protected against larger state shifts (meaning $\hat{S}$-type errors). But, since the total number of available states in any physical system is for practical applications always bounded, a larger spacing always means a smaller protection against phase shift errors of the $\hat{P}$-kind.

As an example of this trade-off, a different encoding of the qubit in the toy model from above could be given by

$$|\bar{0}\rangle = |0\rangle, \tag{3.4a}$$

$$|\bar{1}\rangle = |9\rangle. \tag{3.4b}$$

This encoding is stabilized by $\hat{S}^{18}$ and $\hat{P}^2$ (as can be checked with the same method as above). In this case errors would be detected using the commutation relations of

$$(\hat{S}^a \hat{P}^b)\hat{S}^{18} = \omega^{18b} \hat{S}^b (\hat{S}^a \hat{P}^b) \tag{3.5a}$$

$$(\hat{S}^a \hat{P}^b)\hat{P}^2 = \omega^{2a} \hat{P}^2 (\hat{S}^a \hat{P}^b). \tag{3.5b}$$

In this case the qubit would be protected against errors of $\hat{S}^a$ with $a \in \{-4, -3, ..., 0, ..., 3, 4\}$. But, as can again be seen from equation 3.5, it loses all protection against phase shift errors (since $\omega^{18b} = 1$ for any b). This shows how more protection against one type error, here the shift errors, directly implies less protection against the other type, here phase type errors.

A consequence of this trade-off leads to a central design choice when constructing shift resistant encodings, referred to as the the spacing of the states. How far the states, in the case of the toy model the $|j\rangle$ states, should be apart, has to be decided upon by how the errors in each domain relate. Say a $\hat{P}$-type error happens a tenth of the $\hat{S}$-errors, then we have to construct the code

accordingly by taking a larger shift spacing. Thus in this case the encoding of equation 3.4 would be justified. But if the errors happen with equal probability, the encoding of equation 3.2 would be a better choice.

Logical operators and errors

In order to define the most basic bit operations the logical operators X and Z need to be defined for the encoded states (to obtain the Pauli-group, see chapter 2). In the case of the first encoding (meaning equation 3.2) these logical operators can be encoded as

$$\bar{X} = \hat{S}^3, \bar{Z} = \hat{P}^3. \tag{3.6}$$

Crucially these operators satisfy the commutation relation of

$$\hat{S}^3\hat{P}^3 = -\hat{P}^3\hat{S}^3 \Rightarrow \bar{X}\bar{Z} = -\bar{Z}\bar{X}. \tag{3.7}$$

As was discussed in Chapter 2, these logical operators need to commute with the stabilizers, such that the code remains in the linear subspace stabilized by $\hat{S}^6, \hat{P}^6$ after their application. This does however mean that the shift resistant error protection does not protect against a full "logical error". A logical error, in this setting, is seen as an accumulation of smaller shift errors against which the code is protected. The central idea is that a large enough shift to truly disturb the state would be so unlikely, that the these logical errors are rare enough for all practical purposes.

Other types of errors

In the discussion of the encoding presented by equation 3.2, it was mentioned that this encoding is protected from errors of the type $\hat{S}^a\hat{P}^b$ with $a, b \in \{-1, 0, 1\}$, but the effect of other type of errors was still open. Here we revisit that question. Here two remaining error types are distinguished: large shifts and local shifts. As mentioned in the section above, large shift result in logical errors, and the encoding can neither detect large shifts as errors nor correct them accordingly (since they are interpreted as a logical operation, not as an error). With a local shift an operator is meant which swaps two states and acts on the rest as the identity. As example would be an operator which swaps $|3\rangle$ and $|4\rangle$. The effect of this errors on $|\bar{1}\rangle$ would be $|\bar{1}\rangle_{error} = \frac{1}{\sqrt{3}}(|4\rangle + |9\rangle + |15\rangle)$. The encoding can detected this class of errors, but cannot correct them.

To see the encoding can only detect and not correct the local shift, the difference is shortly discussed here. An error is detectable, if it does not commute with one of the stabilizers. As can can easily be checked, $\hat{E}_{swap,3,4}\hat{P}^6 \neq \hat{P}^6\hat{E}_{swap,3,4}$, thus these local swap errors are detectable. A set of errors is correctable, when all the errors satisfy the so-called Knill-Laflamme conditions (see also [25]). These conditions are given by

$$\langle\bar{0}|\,\hat{E}_i\hat{E}_j\,|\bar{0}\rangle = \langle\bar{1}|\,\hat{E}_i\hat{E}_j\,|\bar{1}\rangle \tag{3.8a}$$

$$\langle\bar{0}|\,\hat{E}_i\hat{E}_j\,|\bar{1}\rangle = \langle\bar{1}|\,\hat{E}_i\hat{E}_j\,|\bar{0}\rangle = 0 \tag{3.8b}$$

for all the errors $\hat{E}_i, \hat{E}_j$ in the set of errors. Adding the local swap errors to the set of correctable errors would not satisfy the first condition (take for example $\hat{E}_i = I$ and $\hat{E}_j = \hat{E}_{swap,3,4}$). Thus a local swap is only detectable. In this case the calculation would have to be restarted. Luckily these local errors often lack a physical meaning and are disregarded in the discussion of a shift resistant encoding.

Conclusions from the toy model

As can be seen from the toy model, to obtain a shift resistant encoding three elements, the qubit, stabilizers and logicals, need to specified. These elements relate in the following way: both of the stabilizers need to act as an identity on the encoded states and the logicals need to act as desired on the encoded state (meaning $\hat{\bar{Z}}\,|0\rangle = |0\rangle$, $\hat{\bar{X}}\,|+\rangle = |+\rangle$, etc.) plus commute with the

stabilizers. These relations lead to there only being one degree of freedom in choosing the shift resistant encoding, namely the spacing of the states. This spacing of the states, which specifies the range of the correctable errors in both the X and Z domains, should be chosen according to the error frequency in each domain. Once this spacing is specified the qubit, stabilizers and logicals can be constructed and the encoding is fixed. For a realistic encoding the states are not as ideal as in this toy model, where every state could be achieved with infinite precision. The last step of the encoding is then to specify a form of approximating the ideal states. This procedure describes the recipe to obtain a shift resistant encoding.

3.2 Encoding in a quantum harmonic oscillator: The GKP code

The most important example of these shift resistant encodings is the so-called the GKP[1] code. The GKP code encodes a qubit in a harmonic oscillator. Here the theoretical construction and practical implementation of the GKP code, following the recipe from above, are discussed. This section is based on [24] and [26].

The setting of the GKP code

The GKP code makes use of the well-known position $\hat{Q}$ and momentum $\hat{P}$ operators. Since both operators are self-adjoint operators, they generate the unitary operators $e^{i\alpha\hat{P}}$ and $e^{i\beta\hat{Q}}$ for any real α, β by Stone's theorem. These operators function in the following way on the eigenstates

$$e^{i\alpha\hat{P}} |p\rangle = e^{i\alpha p} |p\rangle, \tag{3.9a}$$

$$e^{i\beta\hat{Q}} |q\rangle = e^{i\beta q} |q\rangle, \tag{3.9b}$$

and their commutation relation is given by the Weyl relation

$$e^{i\beta\hat{Q}} e^{i\alpha\hat{P}} = e^{-i\alpha\beta} e^{i\alpha\hat{P}} e^{i\beta\hat{Q}}. \tag{3.10}$$

By a smart choice of α and β these operators provide a setting for quantum computation.

As noted in the conclusion of the toy model, the construction of a shift resistant encoding has three related elements, the logicals, the qubit and the stabilizers. The critical requirement for the GKP encoding is that for the logical operators the smart choice of α and β (in the context from above) is given by $\alpha_{logical}\beta_{logical} = \pi$. The ratio of $\alpha_{logical}$ and $\beta_{logical}$ defines the spacing of the states and is chosen according to the ratio of errors in the respective domains. In most practical cases these errors will have the same strength. This will be used as a design requirement in the remainder of this section. In order to get this equal spacing we choose $\alpha_{logical} = \beta_{logical} = \sqrt{\pi}$.

The logical, qubit and stabilizers

With the spacing fixed, the logicals, qubit and stabilizers can be specified. The logicals in this case are given by

$$\hat{\bar{Z}} = e^{i\sqrt{\pi}\hat{Q}}, \tag{3.11a}$$

$$\hat{\bar{X}} = e^{i\sqrt{\pi}\hat{P}} \tag{3.11b}$$

By using the Weyl equation from above and $\alpha\beta = \pi$, these operators obey the commutation relation of

$$\hat{\bar{Z}}\hat{\bar{X}} = -\hat{\bar{X}}\hat{\bar{Z}}. \tag{3.12}$$

[1] After its inventors Daniel Gottesman, Alexei Kitaev, and John Preskill

For these logical operators, the states which satisfy the required eigenvalue relations to represented the qubit, are given by

$$|\bar{0}\rangle = \sum_{k\in\mathbf{Z}} \left|q = 2k\sqrt{\pi}\right\rangle \tag{3.13a}$$

$$|\bar{1}\rangle = \sum_{k\in\mathbf{Z}} \left|q = (2k+1)\sqrt{\pi}k\right\rangle. \tag{3.13b}$$

By using equations 3.9 it can be checked, that these states satisfy the required $\hat{Z}|0\rangle = |0\rangle$ and $\hat{Z}|1\rangle = -|1\rangle$ as well as the required $\hat{X}$ relations, which can be checked by taking the Fourier transform of the states form 3.13 and applying 3.11b.

The second step is to construct the stabilizer measurements. The $2\sqrt{\pi}$ periodicity of the qubit states already hints at the form of the stabilizer. For a general encoding it is required that $\alpha_{stabilizer}\beta_{stabilizer} = 2\pi k$, with $k \in \mathbb{Z}$ $\alpha_{stabilizer} = 2\alpha_{logical}$. Again with the design choice of equal space and choosing $k = 2$, the stabilizer operator are of the following form:

$$\hat{S_Q} = e^{i2\sqrt{\pi}\hat{Q}} \tag{3.14a}$$

$$\hat{S_P} = e^{i2\sqrt{\pi}\hat{P}} \tag{3.14b}$$

These operators would, in the ideal case, detect any deviation from the delta peaks and keep the code perfectly stable.

The approximation of the ideal scenario

The ideal case from equation 3.13 is not very realistic. The states from 3.13 are non-normalizable, they require infinite space and momentum and the creation of delta peaks in space or momentum costs infinite energy. This representation is thus mostly used to understand many of the codes characteristics, but not practically feasible.

In order to achieve a physical representation of these states two approximations are used. The first approximation is to approximate the delta peaks by a small Gaussian function in order to achieve a state which requires finite energy to create, the second is to place over these peaks a Gaussian envelope in order to make the total state normalizable. A crucial property of the Gaussian functions is that they remain Gaussian under the Fourier transform, so the approximation works both in the space and in the momentum domain. The approximate states in this case are given by:

$$\langle x|\bar{0}\rangle = N_0\Big[\sum_{k\in\mathbf{Z}} e^{-\frac{(x-2k\alpha)^2}{2\kappa^2}}\Big]e^{-\frac{x^2}{2\Delta^2}} \tag{3.15a}$$

$$\langle x|\bar{1}\rangle = N_1\Big[\sum_{k\in\mathbf{Z}} e^{-\frac{(x-(2k+1)\alpha)^2}{2\kappa^2}}\Big]e^{-\frac{x^2}{2\Delta^2}} \tag{3.15b}$$

Where N_0, N_1 are normalization constants, κ stands for the width of the Gaussian functions approximating the delta peaks and Δ stands for the width of the overlapping Gaussian function. Here both the values of κ and Δ "cost" energy and are directly responsible for the quality of the approximation. A plot of these approximate states is presented in figure 3.1.

Error modelling

The central motivation of constructing a shift resistant code is that small errors, which in any physical system are accumulated over time, can be detected and corrected. This gives rise to the questions: which errors can be corrected for the GKP encoding? And what error is introduced by the approximation of the ideal states?

First the problem of which errors are correctable. The easiest way to look at this problem is graphically. For this see the figure below.

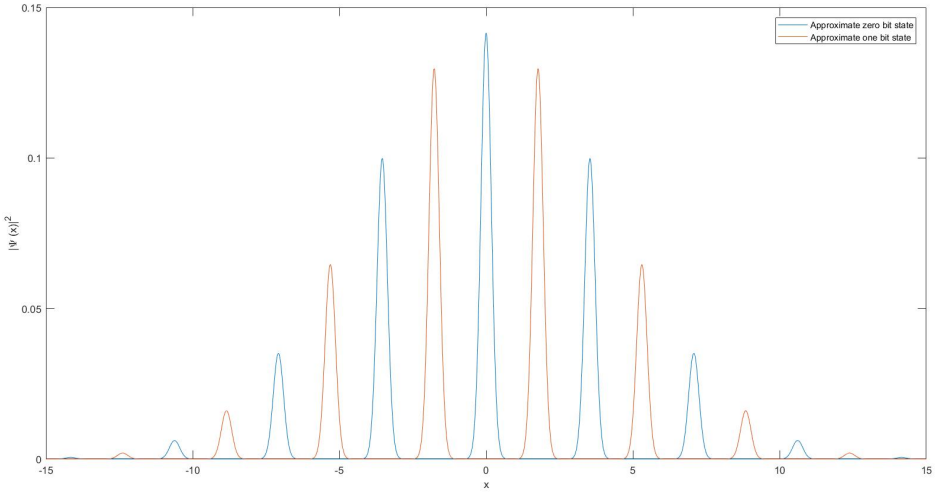

Figure 3.1: The approximate states of the encoding of the zero $|0\rangle$ and one $|1\rangle$ bit in the GKP harmonic oscillator encoding. Here $\alpha = \sqrt{\pi}$, the width of the peaks is given by $\kappa = 0.25$ and is given by the width of the Gaussian envelope $\Delta = 6$.

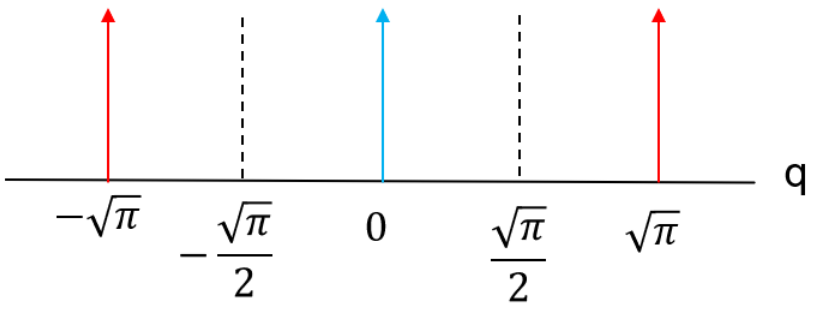

Figure 3.2: A small portion of the q-space in which 3 delta peaks from the ideal GKP states (which are an infinite sum of delta peaks spaced by $\sqrt{\pi}$) are presented. The two red states are part of the 1 bit state, the blue part of the 0 bit state. The dotted line enclosing the blue 0 bit state shows the region of correctable errors for the $|q = 0\rangle$ part of the zero bit state.

Since the ideal states can never be created, for deciding whether the measured outcome is a $|0\rangle$ or a $|1\rangle$ when measuring the position of the state $\hat{Q}$, the following rule is used: if the outcome is closer to an ideal $|0\rangle$-peak then to a $|1\rangle$-peak, the state is a $|0\rangle$ and vice versa. As can be seen in the figure above, any outcome with $q \in (-\frac{\sqrt{\pi}}{2}, \frac{\sqrt{\pi}}{2})$ is considered a $|0\rangle$ state. Since this scheme is repeated periodically, the encoding can protect the state against shifts of $e^{i\hat{\epsilon}P}$ with $|\epsilon| < \frac{\sqrt{\pi}}{2}$. The same idea can be applied in the momentum space, so the encoding is also protected against shift of $e^{i\hat{\delta}Q}$ with $|\delta| < \frac{\sqrt{\pi}}{2}$.

The values above are for an encoding with equal spacing. If there is unequal spacing the correctable errors are $|\epsilon| < \frac{\alpha_{logical}}{2}$ and $|\delta| < \frac{\pi}{2\alpha_{logical}}$. This shows the already mentioned trade-off, a larger spacing in the space domain means more error protection there, but less protection from momentum shift error (and vise versa).

Now in order to calculate the probability of finding the in the wrong state, using the approximation given above, the same idea can be used. Calculating the probability that the particle is outside of the correctable region will provide the error probability of the approximate state. This

means that

$$p_e(|0\rangle) = \sum_{k\in\mathbf{Z}} \int_{(2k+\frac{1}{2})\sqrt{\pi}}^{(2k+1\frac{1}{2})\sqrt{\pi}} \left(N_0 \Big[\sum_{k\in\mathbf{Z}} e^{-\frac{(x-2k\alpha)^2}{2\kappa}} \Big] e^{-\frac{x^2}{2\Delta^2}}) \right)^2 dx. \tag{3.16}$$

By taking $\Delta = \frac{1}{\kappa}$ this error probability is about 1% for $\Delta = 0.5$, but already 10^{-6} for $\Delta = 0.25$. [24]

3.3 Encoding in rotation-symmetric bosonic system

A second important example of shift resistant encoding is given by encoding the qubit using the number of bosons in a harmonic oscillator. The state of the number of bosons is given by two conjugate variables: the number of bosons, measured by the number operator $\hat{n}$, and the phase of the bosons, described by the phase operator $\hat{\phi}$. The main advantage of this encoding that a lot of progress is made in manipulating these bosonic states. The main disadvantage is that the phase operator $\hat{\phi}$ does not exist as a standard quantum mechanical observable and has to be approximated by a POV-measurement (for more on this, see section 1.3). This encoding behaves very similar to the encoding in a rotor space and thus it is fruitful to study this setting in detail.

Again for the construction of an encoding three ingredients are necessary: logical operators, stabilizer measurements and approximated qubit states. Due to the problems of the phase measurement the focus will first be on number eigenspace. Here the logical $\hat{\bar{Z}}$ and its associated stabilizer measurement (in the same way S_q and $\hat{\bar{Z}}$ where related for the GKP code) are constructed, after which the code states for this situation will be introduced. Again these states will be ideal, but non-physical. Given this information the conjugate phase domain will come into the picture and the idealized state will be presented in terms of phase states. Using these idealized states the logical operator $\hat{\bar{X}}$ and stabilizer in the phase domain can be constructed. With all the stabilizer and logical operators done, the approximated states can be made to complete the encoding of the qubit. This section is based on [15].

The idealized encoding

In the previous example the main design choice was given by picking the value of α, which was responsible for the spacing (and thus the level of protection) of the states in both the p- and q-domain. For this encoding, the analogue variable is given by the variable N, which represents the spacing of the number states. The encoding is named a rotation symmetric encoding, this is because the stabilizer in the Z-domain is given by

$$\hat{R_N} = e^{i\frac{2\pi}{N}\hat{n}}, \tag{3.17}$$

where $e^{i\frac{\hat{2}\pi}{N}n}$ is a unitary operator generated by the self-adjoint number operator $\hat{n}$ given by Stone's theorem (see equation 3.9 for how these operator act on the eigenvalues). The qubit is encoded in the subspace of the all states which have a $+1$ eigenvalue, i.e. the states having $n = 0 \bmod N$.

For these states the logical $\hat{\bar{Z}}$ is given by

$$\hat{\bar{Z}} = e^{i\frac{\pi}{N}\hat{n}}. \tag{3.18}$$

In this case the ideal shift resistant qubit encoding is given by

$$|0\rangle = \sum_{n=0}^{\infty} f_{2kN} \, |2kN\rangle, \tag{3.19a}$$

$$|1\rangle = \sum_{n=0}^{\infty} f_{(2k+1)N} \, |(2k+1)N\rangle. \tag{3.19b}$$

This encoding protects against shifts number state shifts V_n, with $V_n \, |k\rangle = |k+1\rangle$ of size $(V_n)^\alpha$ with $\alpha \in \{-\lfloor \frac{N-1}{2} \rfloor, -\lfloor \frac{N-1}{2} \rfloor + 1, ..., \lfloor \frac{N-1}{2} \rfloor\}$. If there would be no conjugate phase domain, this would be the full story and any choice f_{kN} with $\sum_{n=0}^{\infty} |f_{2kN}|^2 = \sum_{n=0}^{\infty} |f_{(2k+1)N}|^2 = 1$ would suffice.

But this is not the case. The states can also obtain phase-errors, against which the protection further specifies the states. The states presented above are represented in the ϕ-domain by

$$|0\rangle = \sum_{m=0}^{2N-1} \left|\phi = \frac{m\pi}{N}\right\rangle, \tag{3.20a}$$

$$|1\rangle = \sum_{m=0}^{2N-1} (-1)^m \left|\phi = \frac{m\pi}{N}\right\rangle, \tag{3.20b}$$

where

$$|\phi\rangle = \frac{1}{\sqrt{2\pi}} \sum_{n=0}^{\infty} e^{in\phi} |n\rangle, \tag{3.21}$$

from which the f_{kN} are specified.

As in the GKP example, these ideal states are non-normalizable. These states do however provide great insight in the structure of the encoding. As can be seen from expression 3.20 the states are protected from "phase" shifts $e^{i\alpha\hat{n}}$ of $|\alpha| < \frac{\pi}{2N}$, which again shows the trade-off made in choosing the value of N. A second use for these expression is their use in defining the logical operator on the conjugate domain given by $\hat{\bar{X}}$. For this choice of f_{kN} the states of $|0\rangle$ and $|1\rangle$ are translation invariant under the operator

$$\hat{\sum_N} = \sum_{m=0}^{2N-1} |m\rangle\langle m+2N| = \hat{S}, \tag{3.22}$$

which is the stabilizer of the conjugate domain phase domain (meaning $\hat{S}|\bar{0}\rangle = |\bar{0}\rangle$ and $\hat{S}|\bar{1}\rangle = |\bar{1}\rangle$). The $\hat{\bar{X}}$ is now given by

$$\hat{\bar{X}} = \sum_{m=0}^{2N-1} |m\rangle\langle m+N|. \tag{3.23}$$

As can be checked on the $|n\rangle$ eigenstates, the logical operators satisfy the required commutation relation of $\hat{\bar{X}}\hat{\bar{Z}} = -\hat{\bar{Z}}\hat{\bar{X}}$. For the encoding to function properly, the approximated states require (under approximation) the same shift-invariance for both stabilizer operators.

Approximated states

In the previous section the idealized states were presented as "phase" eigenstates, which is a sketchy affair since the phase-space is not properly defined. This was said to be the main disadvantage of this encoding. In the approximation of these states this encoding shows its strength. For the approximation there are multiple options which approach $\Delta(\phi) \to 0$ as the available maximum of number-states increases to infinity. In any realistic system these infinite sums would then be approximated by truncated sums. The coefficient f_{kN}, as in equation 3.19, for three encoding options are presented in the table below:

Table 3.1: The coefficient of three approximations for the bosonic encoding. The first column gives their names, with their associated symbol in the second column. In the third column the coefficients f_{kN} are presented, as function of the variable associated with each approximation (α, K and s respectively). The fourth gives the limit for the encoding were the minimal number of states are used, called the trivial encoding. This encoding is easiest to realize, but lacks any error correcting capability. The fifth column is the limit where an infinite number of states are used, which is impossible to realize but can perfectly correct the errors. For the last limit the coefficients f_{kN} are explicitly given in the last column. From [15].

code	$\|\Theta\rangle$	f_{kN}	trivial	limit	limiting f_{kN}
cat	$\|\alpha\rangle$	$\sqrt{\frac{2}{\mathcal{N}_i^*}}\frac{e^{-\|\alpha\|^2/2}\alpha^{kN}}{\sqrt{(kN)!}}$	$\alpha \to 0$	$\alpha \to \infty$	$\left(\frac{2N^2}{\pi\alpha^2}\right)^{\frac{1}{4}} \exp\left[\frac{-(kN-\alpha^2)^2}{4\alpha^2}\right]$
binomial	$\|\Theta^{\text{bin}}_{N,K}\rangle$	$\sqrt{\frac{1}{2^{K-1}}\binom{K}{k}}$	$K = 1$	$K \to \infty$	$\left(\frac{8}{\pi K}\right)^{\frac{1}{4}} \exp\left[\frac{-(k-K/2)^2}{K}\right]$
Pegg-Barnett	$\|\phi = 0\rangle_s$	$\sqrt{2/\lceil s/N \rceil}$	$s = 2$	$s \to \infty$	$\sqrt{2/\lceil s/N \rceil}$

To better understand the functioning of these approximations, it helps to see them in a plotted form. This is presented in the figure below:

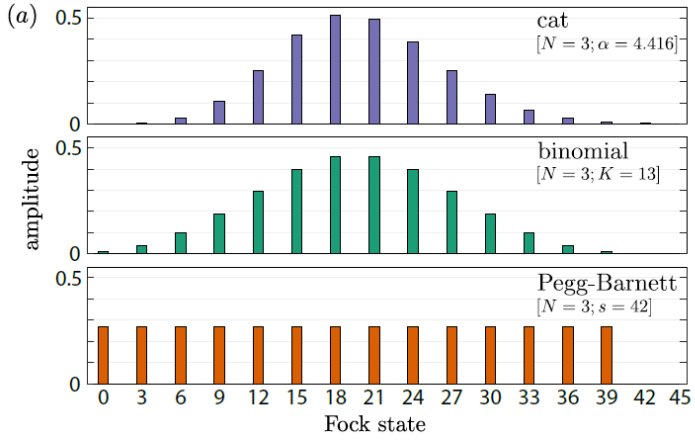

Figure 3.3: The approximation of the state: $\frac{1}{\sqrt{2}}(|0\rangle + |1\rangle)$ by the three different approximations from the table above. The average measured number state, here called a Fock state, is $\langle \hat{n} \rangle = 19.5$ and the spacing of the number, or Fock, states N is given by N = 3 for each of the approximations. the parameters for the respective approximation are given by $\alpha = 4.416$, $K = 13$ and $s = 42$. From [15].

A first note on these approximations is that, as seen in the GKP encoding, two of the approximations again approach a Gaussian profile as the quality of the approximation increases. A second note is that as the quality, represented by parameters α, K and s respectively increase, the energy cost to realize the approximation increases. The relation between the number of available number states increases and the quality of the approximation of $\Delta(\phi) \to 0$, is given in the figure below.

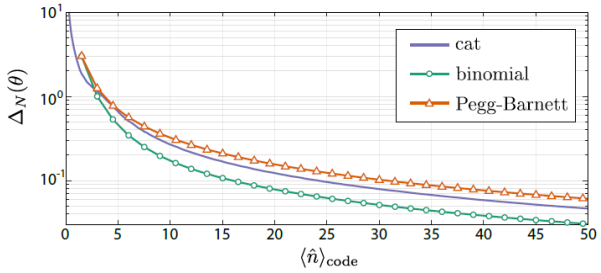

Figure 3.4: The uncertainty in the phase domain, here denoted by $\Delta_N(\theta)$, as a function of $\langle \hat{n} \rangle$ for the three different approximations of table 3.1. The states approximate the state of $\frac{1}{\sqrt{2}}(|0\rangle + |1\rangle)$. For this approximation the spacing between the numberstates is taken to be N = 3 and the parameters for the approximation are as in figure 3.3, meaning $\alpha = 4.416$, $K = 13$ and $s = 42$. From [15].

Conclusion

In this chapter the concept of a shift resistant encoding was introduced. This encoding makes use of two conjugate variables connected by the Fourier transform. The encoding protects the qubit against small shift error in both domains. The ratio of the probabilities of the errors in both domains leads to an optimal spacing coefficient, on which the whole design of the encoding is based. For this spacing coefficient the stabilizer, logical operators and an ideal representation of the qubit can be specified. Since a system can never be kept in the ideal state, for which the encoding is

protected against both error types, the last step is to find a suitable, implementable approximation to complete the encoding. These encodings then form the basis of a quantum computation scheme, with error correcting properties build into the design of the hardware.

4. Quantum computation in a rotor system

In this chapter one of the main results of this report is presented, a quantum computing scheme for a quantum mechanical rotor system. But our goal is not only to achieve quantum computation, but to theoretically design this in way that it is resistant to small shift errors on the system. This goal is first achieved on the level on the encoding of the qubits, by presenting a shift resistant encoding (for more on shift resistant encodings, see the previous chapter). With this encoding small errors can be detected by using the stabilizers, without disturbing the state of the . Presenting this encoding will form the first part of this chapter. This resistance to small errors is also taken to the level of the quantum gates. The gates are designed to commute with the correctable errors, thus making it possible to correct the errors at any stage during the computation. The presentation of the error resistant gates forms the second part of this chapter.

4.1 Encoding a qubit in a rotor

In this section the shift resistant encoding of the qubit in a rotor system is presented. A shift resistant encoding has three parts: logicals, the stabilizers and the representation of the qubit. As noted in the previous chapter, a shift resistant encoding is fixed by the spacing between the representing states. The encoding in a rotor takes its simplest form when taking a spacing between the angular momentum states of zero, therefore this case is first discussed in an idealized, but unrealistic, form. This encoding is then expanded to an encoding for any angular momentum spacing, which forms the second part of this section. In order to obtain a realistic encoding the last part of this section focuses on approximating the idealized encodings as mentioned before. This section is based on [9].

The ideal encoding for "zero" angular momentum spacing

This encoding assumes that errors in the angular momentum space happen with negligible probability and offers no protection to these errors. It however provides maximal protection against shifts in the angular position, up to shifts of $\frac{\pi}{2}$. Since the encoding assumes no angular momentum errors, the even and odd integer angular momentum states are used to encode the qubit. For "zero" spacing this gives an idealized representation of

$$|\bar{0}\rangle = \sum_{l\in\mathbb{Z}} |2l\rangle\,, \tag{4.1a}$$

$$|\bar{1}\rangle = \sum_{l\in\mathbb{Z}} |2l+1\rangle\,. \tag{4.1b}$$

As mentioned in chapter 1, the states in the angular momentum domain of $\hat{L}$ and the angular position of $\hat{\Theta}$ are related by the discrete Fourier transform. By taking this discrete Fourier transform on the states above, the states are expressed in the angular position space by

$$|\bar{0}\rangle = |\theta = 0\rangle + |\theta = \pi\rangle\,, \tag{4.2a}$$

$$|\bar{1}\rangle = |\theta = 0\rangle - |\theta = \pi\rangle\,. \tag{4.2b}$$

For these states the logical operations and stabilizers can be specified. The logical $\hat{\bar{Z}}$ is given by

$$\hat{\bar{Z}} = e^{i\pi\hat{L}} \tag{4.3}$$

and the stabilizer associated with this operator is given by

$$\hat{S_L} = e^{i2\pi\hat{L}}. \tag{4.4}$$

These operations represent rotations of the system over the angle π (radians) for $\hat{\bar{Z}}$ and 2π for the stabilizer. Thus the stabilizer for zero spacing leaves the whole angular momentum space unchanged. Because it is assumed that there are no errors in the angular momentum states, the stabilizer does not need to detect any errors.

For the construction of the $\hat{\bar{X}}$ operator two options exist. The two candidate operators are given by

$$\hat{\bar{X}} = \hat{V} \tag{4.5a}$$

$$\hat{\bar{X}} = \frac{1}{2}((\hat{I} + \hat{\bar{Z}})\hat{V}^\dagger + \hat{V}(\hat{I} + \hat{\bar{Z}})). \tag{4.5b}$$

Both form valid options, since both satisfy the required commutation relation of $\hat{X}\hat{Z} = -\hat{Z}\hat{X}$ and perform the required state operations on the encoded states. The difference is that the latter has the advantage of satisfying the property of $\hat{\bar{X}}^2 = \hat{I}$ in any case, while the former only satisfies this property on the subspace of the ideal encoding. The first on the other hand has a much simpler form, which can lead to an easier implementation.

In any case the stabilizer is given by

$$\hat{S_\theta} = \hat{V}^2. \tag{4.6}$$

This stabilizer is used to correct the only allowed errors in this case, shifts in angular position given by $e^{i\alpha\hat{L}}$. These errors can be detected using the commutation relation (from Chapter 1)

$$\hat{V}^2 e^{i\alpha\hat{L}} = e^{-i2\alpha} e^{i\alpha\hat{L}}\hat{V}^2 \tag{4.7}$$

and are corrected by making the smallest shift needed to re-obtain a $+1$ eigenvalue for the stabilizer $\hat{S_\theta}$. Thus in this case errors can be corrected with $|\alpha| < \frac{\pi}{2}$, as was claimed above. Any shift larger than this range, meaning $|\alpha| > \frac{\pi}{2}$, results in a logical error.

The ideal encoding for non-zero spacing

The encoding above assumes that shifts in angular momentum happen only with a negligible probability. When this is not the case, the encoding has to be protected against these shifts. The encoding presented here is protected against shifts of

$$\hat{V}^n,\ n \in \left\{ \left\lfloor \frac{-N+1}{2} \right\rfloor, -\left\lfloor \frac{-N+2}{2} \right\rfloor, ..., \left\lfloor \frac{N-1}{2} \right\rfloor \right\}. \tag{4.8}$$

with N an odd integer. There are two things to note about the set above. First is that the set above always has size N. Second is that the "zero" spacing case corresponds to the case of $N = 1$ and in this case only $\hat{V}^0 = I$ is a correctable error (thus no actual shift errors can be corrected for, as is in line with what was mentioned above).

The qubit is here encoded as

$$|\bar{0}\rangle = \sum_{l\in\mathbb{Z}} |2Nl\rangle = \sum_{m=0}^{2N-1} \left|\theta = \frac{m\pi}{N}\right\rangle \tag{4.9a}$$

$$|\bar{1}\rangle = \sum_{l\in\mathbb{Z}} |2Nl+N\rangle = \sum_{m=0}^{2N-1} (-1)^m \left|\theta = \frac{m\pi}{N}\right\rangle. \tag{4.9b}$$

Here we interpreted a state in between the $|Nl\rangle$ states as the encoded state it is closest to and correct it by applying angular momentum shifts accordingly.

For the logical $\hat{Z}$ operator there are two possible candidates, given by

$$\hat{\bar{Z}} = e^{i\frac{\pi}{N}\hat{L}} \text{ or} \tag{4.10a}$$

$$\hat{\bar{Z}} = e^{i\lfloor\frac{\hat{L}}{N}\rfloor\pi} \tag{4.10b}$$

Where the first option is easier to implement, but single shifts can influence the logical state of the qubit, meaning that $\hat{V}\hat{\bar{Z}}\hat{V}^\dagger \neq \hat{\bar{Z}}$. The second option is error resistant to small shifts, but is harder to implement then the first (because of the $\lfloor\frac{\hat{L}}{N}\rfloor$ operator). In any case the stabilizer is given by

$$\hat{S_L} = e^{i\frac{2\pi}{N}\hat{L}}. \tag{4.11}$$

Associated to each of the options from above a logical $\hat{X}$ operator can be constructed. These two options are given by

$$\hat{\bar{X}} = \hat{V}^N \text{ or} \tag{4.12a}$$

$$\hat{\bar{X}} = \frac{1}{2}((\hat{I}+\hat{\bar{Z}})\hat{V}^{\dagger N} + \hat{V}^N(\hat{I}+\hat{\bar{Z}})), \tag{4.12b}$$

where 4.12a is related to 4.10a, sharing the easy to implementation, and 4.12b is related to 4.10b (in the sense of being small shift error resistant). In this case there is no clear preference between the two, since it depends on how achievable to the second option is for the physical system in which the encoding is implemented. In any case the stabilizer is given by

$$\hat{S_\theta} = \hat{V}^{2N}. \tag{4.13}$$

This completes the encoding in a rotor space.

The approximate encodings and error analysis

As seen before in chapter 3 the states used here to encode the qubit are nonphysical. The states are non-normalizable in the angular momentum space and represented by impossible to realize delta-peaks in the angular position space. Thus in order to realize the scheme presented above, these states need to be approximated.

Since the angular position variable θ is a continuous variable (as opposed to the angular momentum being discrete), the approximation is easiest done in the angular position space. For the approximation any sharply peaked, periodic function (with period 2π) will suffice. Two examples are given by

$$|\theta = \theta_0\rangle = N_0 \int_0^{2\pi} \sum_{m\in\mathbb{Z}} e^{-\frac{\xi^2}{2}(\theta-\theta_0+m2\pi)^2} |\theta\rangle\, d\theta \text{ and} \tag{4.14a}$$

$$|\theta = \theta_0\rangle = N_1 \int_0^{2\pi} cos^\gamma(\frac{\theta-\theta_0}{2}) |\theta\rangle\, d\theta \tag{4.14b}$$

Where N_1 and N_1 are normalization constants and both the parameters ξ and γ are responsible for the quality of the approximation.[1] The representation of the states in the angular momentum states is obtained by taking the Fourier transform.

The errors induced by this approximation are also best calculated in the angular position space. For the logical $\hat{X}$ (ideal) eigenstates $|+\rangle$ and $|-\rangle$ this is done most easily, since they are represented

[1] Note that the first example is not in $[0, 2\pi]$, on the whole of $\mathbb{R}$. Since $e^{-\xi^2}$ is in it itself not a periodic function the function is repeated here to still represent periodic function.

by a single delta-peak of $|+\rangle = |\theta = 0\rangle$ and $|-\rangle = |\theta = \pi\rangle$ in the case of zero spacing. For these eigenstates the following projection method is used: the state is interpreted to be the delta peak it is closest to (compare this to the GKP code in 3.2). This method divides the $[0, 2\pi]$ angular position space into equal parts representing the $|+\rangle$ and $|-\rangle$ states, which is graphically represented in the figure below.

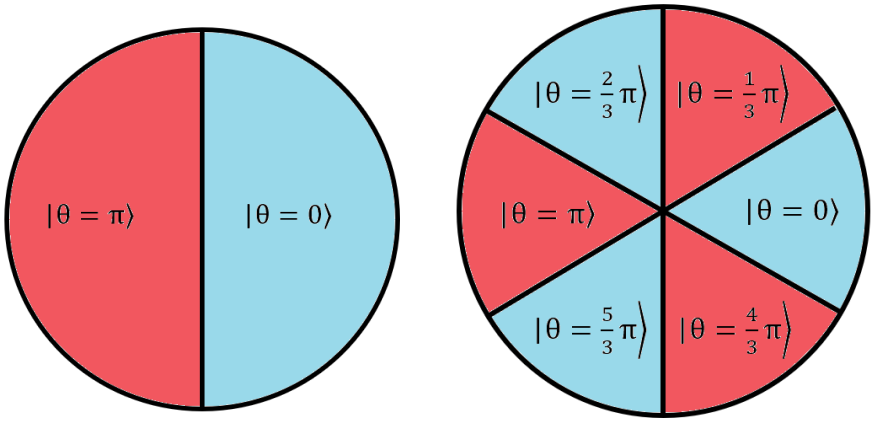

Figure 4.1: The error correcting states projection in the angular position domain for N = 1 in (a) and N = 3 in (b).

Equipped with this state projection method, the errors introduced by the approximation can be calculated. This is simply done by calculating the probability of finding the states on the other side of the division. This means that if the state should, for example, be in the $|+\rangle$ state for a spacing of $N = 1$, the error is calculated by the probability of finding the angular position in the state denoted by the red parts of figure 4.1(a). Thus let $\Psi_+(\theta) = \langle\theta|+\rangle$ be the approximation of the $|+\rangle = |\theta = 0\rangle$ state, then the error introduced by the approximation is given by

$$p_e(|+\rangle) = \int_{-\pi}^{-\frac{\pi}{2}} |\Psi_+(\theta)|^2 d\theta + \int_{\frac{\pi}{2}}^{\pi} |\Psi_+(\theta)|^2 d\theta \tag{4.15}$$

and in similar manner for $|-\rangle$ the error is given by

$$p_e(|-\rangle) = \int_{-\frac{\pi}{2}}^{\frac{\pi}{2}} |\Psi_-(\theta)|^2 d\theta. \tag{4.16}$$

With these expressions the error in any superposition can be calculated by expressing the superposition in the $|+\rangle$ and $|-\rangle$ basis.

As holds for general shift resistant encodings, making the spacing (and thus error resistance) in one domain larger the spacing in the other domain decreases. Here we see that by making the spacing between the angular position larger the part of the circle representing an ideal angular position peak gets smaller. As an example using the setting from figure 4.1, for zero spacing, which corresponds to $N = 1$ in the context of equation 4.9, the angular position $|\theta = 0\rangle$ has any state between $\left|\theta = -\frac{\pi}{2}\right\rangle$ and $\left|\theta = \frac{\pi}{2}\right\rangle$ to represent it. If the spacing is increased to $N = 3$ (again in the context of 4.9) the angular position state $|\theta = 0\rangle$ is only represented by state between $\left|\theta = -\frac{\pi}{6}\right\rangle$ and $\left|\theta = \frac{\pi}{6}\right\rangle$. This range of angular position states used to approximate an ideal peak is referred to as the correctable error range (in the angular position domain). The correctable error range scales with the spacing as $\frac{\pi}{N}$. This correctable error range corresponds to protection against angular position shifts scales of $e^{i\alpha\hat{L}}$ with $|\alpha| < \frac{\pi}{2N}$. This shows the 'cost' of increasing the spacing in the angular momentum domain.

4.2 Quantum gates for the rotor space

In this section the complete set of quantum gates for the rotor encoding are presented. Here the complete set is given by the gates discussed in chapter 2, meaning the gates

$$\{\hat{C}_{rot}, \hat{H}, \hat{S}\} \cup \{\hat{T}\}. \tag{4.17}$$

First the gates are introduced for the setting where the spacing between the angular momentum states is zero, meaning all even states encode $|\bar{0}\rangle$ and all uneven states encodes $|\bar{1}\rangle$. These are then generalized to serve as gates for any spacing between the states.

The gates presented here are designed to be resistant to the correctable errors, by which we mean that the occurrence of a correctable error does not alter the effect of the gate. This propery is referred to here as 'small shift error resistant'. This concept is not quite the same as fault-tolerance, which requires a quantification of the error probability and that is absent here, but the concepts of fault-tolerance and small shift error resistance are very closely related. (For more on the precise, formal meaning of fault-tolerance, see [27].)

4.2.1 The gate set for N = 1

For the construction of these gates we note that the $\hat{L_1}$-operator denotes the angular momentum operator for the first qubit and $\hat{L_2}$ the angular momentum for the second. The gates are presented in order of 4.17.

Controlled rotation gate

The $\hat{C}_{rot}$ for this encoding is given by

$$\hat{C}_{rot} = e^{i\pi \hat{\hat{L}_1} \hat{L_2}} \tag{4.18}$$

By letting $\hat{C}_{rot}$ act on a angular momentum eigenstate, the gates acts as

$$\hat{C}_{rot} |l_1\rangle |l_2\rangle = e^{i\pi \hat{L_1} \hat{L_2} 1} |l_1\rangle |l_2\rangle = e^{i\pi l_1 l_2} |l_1\rangle |l_2\rangle = (-1)^{l_1 l_2} |l_1\rangle |l_2\rangle . \tag{4.19}$$

The desired characteristic of the gate is given by

$$(-1)^{l_1 l_2} = \begin{cases} -1, & \text{if } l_1 \text{ and } l_2 \text{ odd,} \\ 1, & \text{else.} \end{cases} \tag{4.20}$$

This makes the gate only induce a phase shift if both states are in $|\bar{1}\rangle$, proving the desired effect.

The Hadamard gate

The Hadamard gate is the hardest to construct in this setting, since it is the only non-diagonal matrix of the four gates. Thereby the Hadamard gate is introduced using a qubit teleportation scheme, this means that the original qubit is measured and its information transplanted on an ancilla (or 'helper') qubit. The implementation of the the Hadamard gate is schematically given in the figure below.

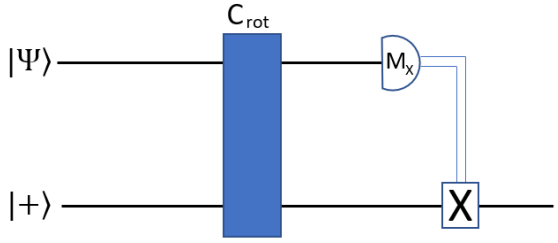

Figure 4.2: Schematic implementation of the Hadamard gate using a qubit teleportation scheme.

To prove this scheme take an arbitrary state, $|\Psi\rangle = \alpha|0\rangle + \beta|1\rangle$. The two qubit state can then be expressed as

$$|\Psi_{start}\rangle = |\Psi\rangle|+\rangle = \frac{1}{\sqrt{2}}(\alpha|0\rangle|0\rangle + \alpha|0\rangle|1\rangle + \beta|1\rangle|0\rangle + \beta|1\rangle|1\rangle). \tag{4.21}$$

where the $|\Psi\rangle$ is in the first Hilbert space and the $|+\rangle$ in the second. Now we apply $\hat{C}_{rot}$ and reorder results in

$$\begin{aligned}\hat{C}_{rot}|\Psi_{start}\rangle &= \frac{1}{\sqrt{2}}(\alpha|0\rangle|0\rangle + \alpha|0\rangle|1\rangle + \beta|1\rangle|0\rangle - \beta|1\rangle|1\rangle)\\ &= \frac{1}{2}(\alpha(|-\rangle|0\rangle + |+\rangle) + \alpha(|-\rangle + |+\rangle)|0\rangle + \beta(|-\rangle - |+\rangle)|1\rangle - \beta(|-\rangle - |+\rangle))|1\rangle\\ &= \frac{1}{2}(|+\rangle(\alpha(|0\rangle + |1\rangle) + \beta(|0\rangle - |1\rangle)) + |-\rangle(\alpha(|0\rangle + |1\rangle) - \beta(|0\rangle - |1\rangle)))\end{aligned} \tag{4.22}$$

Now when measuring in the X-basis on the first qubit, two options arise. The first option is that $|+\rangle$ is measured. This directly gives the required state on the second qubit.

$$\frac{1}{2}(\alpha(|0\rangle + |1\rangle) + \beta(|0\rangle - |1\rangle)) = \frac{1}{\sqrt{2}}(\alpha|+\rangle + \beta|-\rangle) \tag{4.23}$$

The second option is for when $|-\rangle$ is found. To obtain the required state in this case the X-operator is applied to the second qubit. This gives the required state:

$$X\frac{1}{2}(\alpha(|0\rangle + |1\rangle) - \beta(|0\rangle - |1\rangle)) = \frac{1}{2}(\alpha(|1\rangle + |0\rangle) - \beta(|1\rangle - |0\rangle)) = \frac{1}{\sqrt{2}}(\alpha|+\rangle + \beta|-\rangle), \tag{4.24}$$

which shows how the schematic applies the Hadamard gate. The measurement in the X-basis is easiest done in terms of a angular position measurement, after which a controlled angular momentum shift operation (as $\hat{\tilde{X}}$) is performed as described above.

The phase and T gate

The phase gate $\hat{S}$ and magic T gate $\hat{T}$ act as diagonal matrices and thus are much easier to implement. Since the phase gate is simply the $\hat{T}$-gate applied twice, we only show how to implement the $\hat{T}$ gate, but an expression is provided for both

$$\hat{T} = e^{i\frac{\pi}{4}\hat{L}}e^{-i\frac{\pi}{2}\lfloor\frac{\hat{L}}{2}\rfloor}, \tag{4.25a}$$

$$\hat{S} = e^{i\frac{\pi}{2}\hat{L}}e^{-i\pi\lfloor\frac{\hat{L}}{2}\rfloor}. \tag{4.25b}$$

In order to prove the desired functioning of the $\hat{T}$-gate it is noted that the function acts on l modulo 8 ($e^{i\frac{\pi}{4}l} = e^{i\frac{\pi}{4}(l+8)}$). The desired behaviour can be seen, by looking at the effect both operator have on these residue classes. This gives the following relations:

$$e^{i\frac{\pi}{4}l} = \begin{cases} 1, & l \equiv 0 \ mod\ 8 \\ e^{i\frac{\pi}{4}}, & l \equiv 1 \ mod\ 8 \\ i, & l \equiv 2 \ mod\ 4 \\ ie^{i\frac{\pi}{4}}, & l \equiv 3 \ mod\ 8 \\ -1, & l \equiv 4 \ mod\ 8 \\ -e^{i\frac{\pi}{4}}, & l \equiv 5 \ mod\ 8 \\ -i, & l \equiv 6 \ mod\ 8 \\ -ie^{i\frac{\pi}{4}}, & l \equiv 7 \ mod\ 8 \end{cases} \tag{4.26a}$$

$$e^{-i\frac{\pi}{2}\lfloor\frac{l}{2}\rfloor} = \begin{cases} 1, & l \equiv 0,1 \ mod\ 8 \\ -i, & l \equiv 2,3 \ mod\ 8 \\ -1, & l \equiv 4,5 \ mod\ 8 \\ i, & l \equiv 6,7 \ mod\ 8 \end{cases} \tag{4.26b}$$

Now by multiplication it is obtained, that

$$e^{i\frac{\pi}{4}l}e^{-i\frac{\pi}{2}\lfloor\frac{l}{2}\rfloor}|l\rangle = \begin{cases} |l\rangle, & l \ even, \\ e^{i\frac{\pi}{4}}|l\rangle, & l \ uneven. \end{cases} \tag{4.27}$$

The $\hat{S}$ gate can be derived in similar fashion and thus is omitted here, but do also note that $\hat{T}^2 = \hat{S}$. This completes the universal gate set.

As a last note, it is remarked that these gates are small shift error resistant. Since only errors in the angular position space are allowed for the case of $N = 1$, we note that three of the gates are of the $e^{i\alpha\hat{L}}$ form. For the Hadamard gate it is noted that the measurement in $\hat{\tilde{X}}$-basis spans the the whole correctable error range, thus this gate is also fault tolerant for the correctable angle errors.

4.2.2 The gate set for general N spacing

The gates given above are now easily extended to an encoding with spacing N. This encoding protects the code against shift errors as in equation 4.8. To prove the fault tolerance of the gates against shift error, it is used that for these angular momentum shifts of size n the following relation holds

$$\left\lfloor \frac{n + \lfloor\frac{N}{2}\rfloor}{N} \right\rfloor = 0 \tag{4.28}$$

This is used to prove the shift tolerance of the N-spaced gates. The gates are still tolerant to angle errors by the same argument as presented above (only the correctable range diminishes as noted above), so only the resistance to shift errors needs to be proven.

The Controlled rotation gate

The shift tolerant $\hat{C}_{rot}$ gate for N spacing is given by

$$\hat{C}_{rot,N} = \big[\hat{V_1}^{\lfloor\frac{N}{2}\rfloor} \otimes \hat{V_2}^{\lfloor\frac{N}{2}\rfloor}\big]^\dagger e^{i\pi\lfloor\frac{\hat{L_1}}{N}\rfloor\lfloor\frac{\hat{L_2}}{N}\rfloor}\big[\hat{V_1}^{\lfloor\frac{N}{2}\rfloor} \otimes \hat{V_2}^{\lfloor\frac{N}{2}\rfloor}\big]. \tag{4.29}$$

Here $\hat{V_1}, \hat{L_1}$ act on the first Hilbert and $\hat{V_2}, \hat{L_2}$ act on the second Hilbert space. Since for both qubits most likely the same physical representation is used, their (angular momentum) spacing (in the context of equation 4.9) is taken to both be N.

In order to obtain a small shift error resistant $\hat{C}_{rot}$-gate we require that if the encoded state obtains a shift error $\hat{V_1}^n\hat{V_2}^m$ within the correctable error range as in equation 4.8, the action of the gate is the same as on the state without any error. The states, on which such an error has occurred, are of the form $\hat{V_1}^n\hat{V_2}^m|kN\rangle|lN\rangle = |kN+n\rangle|lN+m\rangle$ (with n, m in the correctable range of shift errors). Here we can not take $m = n$, since both system can obtain errors independently.

The $\hat{C}_{rot}$ gate presented above fulfills this requirement of acting the same on $|kN+n\rangle|lN+m\rangle$,

for any n, m within the correctable shift error range. This is shown as follows:

$$\begin{aligned}
\hat{C}_{rot,N}\left|kN+n\right\rangle\left|lN+m\right\rangle &= \left[\hat{V}_1^{\left\lfloor\frac{N}{2}\right\rfloor}\otimes\hat{V}_2^{\left\lfloor\frac{N}{2}\right\rfloor}\right]^\dagger e^{i\pi\lfloor\frac{\hat{L_1}}{N}\rfloor\lfloor\frac{\hat{L_2}}{N}\rfloor}\left[\hat{V}_1^{\left\lfloor\frac{N}{2}\right\rfloor}\otimes\hat{V}_2^{\left\lfloor\frac{N}{2}\right\rfloor}\right]\left|kN+n\right\rangle\left|lN+m\right\rangle \\
&= \left[\hat{V}_1^{\left\lfloor\frac{N}{2}\right\rfloor}\otimes\hat{V}_2^{\left\lfloor\frac{N}{2}\right\rfloor}\right]^\dagger e^{i\pi\lfloor\frac{\hat{L_1}}{N}\rfloor\lfloor\frac{\hat{L_2}}{N}\rfloor}\left]\left|kN+\left\lfloor\frac{N}{2}\right\rfloor+n\right\rangle\right|lN+\left\lfloor\frac{N}{2}\right\rfloor+m\right\rangle \\
&= \left[\hat{V}_1^{\left\lfloor\frac{N}{2}\right\rfloor}\otimes\hat{V}_2^{\left\lfloor\frac{N}{2}\right\rfloor}\right]^\dagger e^{i\pi\lfloor\frac{kN+\left\lfloor\frac{N}{2}\right\rfloor+n}{N}\rfloor\lfloor\frac{lN+\left\lfloor\frac{N}{2}\right\rfloor+m}{N}\rfloor}\left|kN+\left\lfloor\frac{N}{2}\right\rfloor+n\right\rangle\right|lN+\left\lfloor\frac{N}{2}\right\rfloor+m\right\rangle \\
&= e^{i\pi\lfloor\frac{kN+\left\lfloor\frac{N}{2}\right\rfloor+n}{N}\rfloor\lfloor\frac{lN+\left\lfloor\frac{N}{2}\right\rfloor+m}{N}\rfloor}\left[\hat{V}_1^{\left\lfloor\frac{N}{2}\right\rfloor}\otimes\hat{V}_2^{\left\lfloor\frac{N}{2}\right\rfloor}\right]^\dagger\left|kN+\left\lfloor\frac{N}{2}\right\rfloor+n\right\rangle\right|lN+\left\lfloor\frac{N}{2}\right\rfloor+m\right\rangle \\
&= e^{i\pi\lfloor\frac{kN+\left\lfloor\frac{N}{2}\right\rfloor+n}{N}\rfloor\lfloor\frac{lN+\left\lfloor\frac{N}{2}\right\rfloor+m}{N}\rfloor}\left|kN+n\right\rangle\left|lN+m\right\rangle \\
&= e^{i\pi(k+\lfloor\frac{\left\lfloor\frac{N}{2}\right\rfloor+n}{N}\rfloor)(l+\lfloor\frac{\left\lfloor\frac{N}{2}\right\rfloor+m}{N}\rfloor)}\left|kN+n\right\rangle\left|lN+m\right\rangle \\
&= e^{i\pi kl}\left|kN+n\right\rangle\left|lN+m\right\rangle
\end{aligned} \tag{4.30}$$

Where in the second to last step equation 4.28 is used. Since the last form mirrors that of equation 4.20, the $\hat{C}_{rot}$-gate acts as desired and the gate is unaffected by angular momentum shift within the correctable error range. This proves the claimed fault tolerant behaviour of the gate.

An alternative option for a $\hat{C}_{rot}$ would be given by

$$\hat{C}_{rot} = e^{i\pi\frac{\hat{L}_1\hat{L}_2}{N^2}}. \tag{4.31}$$

This gate is much simpler in form than the gate from equation 4.29, which most likely leads a simpler implementation, and acts as desired on the encoded states in equation 4.9, since $e^{i\pi\frac{\hat{L}_1\hat{L}_2}{N^2}}\left|kN\right\rangle\left|lN\right\rangle = e^{i\pi kl}\left|kN\right\rangle\left|lN\right\rangle$. This gate does however alter its effect if the encoded state obtained a shift error. Even an encoded with the error of $\hat{V}_1$ already shows this,

$$\hat{C}_{rot}\hat{V}_1\left|kN\right\rangle\left|lN\right\rangle = e^{i\pi\frac{\hat{L}_1\hat{L}_2}{N^2}}\left|kN+1\right\rangle\left|lN\right\rangle = e^{i\pi\frac{kN+1}{N}l}\left|kN+1\right\rangle\left|lN\right\rangle \neq e^{i\pi kl}\left|kN+1\right\rangle\left|lN\right\rangle. \tag{4.32}$$

Thus this gate is not small shift resistant.

The Hadamard gate

For the Hadamard gate the same argument as above is used. We first note here that the $\hat{C}_{rot}$-gate is shown to be fault tolerant. Secondly we note that the measurement in the $\hat{X}$-basis is a measurement in the angle domain. The outcome of this measurement is not affected by angular momentum state shifts, which acts as phase shifts in the angular position space and thereby does not affect the measurement. This means that the teleportation scheme from above still works small shift error resistantly. Do however note that the correctable angle shift range is now reduced due to the larger angular position spacing (for more on the correctable range see the section on error analysis from above).

The Phase and magic T gate

For the Phase and magic T gates a trick very similar to the $\hat{C}_{rot}$-gate is used. Their expression for a spacing of N now looks the following:

$$\hat{T} = [\hat{V}^{\lfloor\frac{N}{2}\rfloor}]^\dagger e^{i\frac{\pi}{4}\lfloor\frac{\hat{L}}{N}\rfloor}e^{-i\frac{\pi}{2}\lfloor\frac{\lfloor\frac{\hat{L}}{N}\rfloor}{2}\rfloor}\hat{V}^{\lfloor\frac{N}{2}\rfloor} \tag{4.33a}$$

$$\hat{S} = [\hat{V}^{\lfloor\frac{N}{2}\rfloor}]^\dagger e^{i\frac{\pi}{2}\lfloor\frac{\hat{L}}{N}\rfloor}e^{-i\pi\lfloor\frac{\lfloor\frac{\hat{L}}{N}\rfloor}{2}\rfloor}\hat{V}^{\lfloor\frac{N}{2}\rfloor} \tag{4.33b}$$

Here again we require the gate to produce the same effect even if a shift error $\hat{V}^n$, which is in the set of the correctable shift error range as in equation 4.8, has occurred. We prove the effect

of the $\hat{T}$-gate by letting it act on the state on which an such an error has occurred, given by $\hat{V}^n |kN\rangle = |kN + n\rangle$. This gives:

$$\begin{aligned}
\hat{T}|kN+n\rangle = \; & = [\hat{V}^{\lfloor \frac{N}{2} \rfloor}]^\dagger e^{i\frac{\pi}{4}\lfloor \frac{\hat{L}}{N} \rfloor} e^{-i\frac{\pi}{2}\lfloor \frac{\lfloor \frac{\hat{L}}{N} \rfloor}{2} \rfloor} \hat{V}^{\lfloor \frac{N}{2} \rfloor} |kN+n\rangle \\
& = [\hat{V}^{\lfloor \frac{N}{2} \rfloor}]^\dagger e^{i\frac{\pi}{4}\lfloor \frac{\hat{L}}{N} \rfloor} e^{-i\frac{\pi}{2}\lfloor \frac{\lfloor \frac{\hat{L}}{N} \rfloor}{2} \rfloor} \left| kN + \left\lfloor \frac{N}{2} \right\rfloor + n \right\rangle \\
& = [\hat{V}^{\lfloor \frac{N}{2} \rfloor}]^\dagger e^{i\frac{\pi}{4}\lfloor \frac{kN+\lfloor \frac{N}{2} \rfloor+n}{N} \rfloor} e^{-i\frac{\pi}{2}\lfloor \frac{\lfloor \frac{kN+\lfloor \frac{N}{2} \rfloor+n}{N} \rfloor}{2} \rfloor} \left| kN + \left\lfloor \frac{N}{2} \right\rfloor + n \right\rangle \\
& = e^{i\frac{\pi}{4}\lfloor \frac{kN+\lfloor \frac{N}{2} \rfloor+n}{N} \rfloor} e^{-i\frac{\pi}{2}\lfloor \frac{\lfloor \frac{kN+\lfloor \frac{N}{2} \rfloor+n}{N} \rfloor}{2} \rfloor} |kN+n\rangle \\
& = e^{i\frac{\pi}{4}(k+\lfloor \frac{\lfloor \frac{N}{2} \rfloor+n}{N} \rfloor)} e^{-i\frac{\pi}{2}(\lfloor \frac{k+\lfloor \frac{\lfloor \frac{N}{2} \rfloor+n}{N} \rfloor}{2} \rfloor)} |kN+n\rangle \\
& = e^{i\frac{\pi}{4}k} e^{-i\frac{\pi}{2}\lfloor \frac{k}{2} \rfloor)} |kN+n\rangle
\end{aligned} \tag{4.34}$$

Which acts as desired by the same argument as in equation 4.27. Concluding the small shift resistant gate set for an N spaced encoding.

Conclusion

As a small recap: the ideal shift resistant encoding of the rotor space is given by

$$|\bar{0}\rangle = \sum_{l\in\mathbb{Z}} |2Nl\rangle = \sum_{m=0}^{2N-1} \left| \theta = \frac{m\pi}{N} \right\rangle,$$

$$|\bar{1}\rangle = \sum_{l\in\mathbb{Z}} |2Nl+N\rangle = \sum_{m=0}^{2N-1} (-1)^m \left| \theta = \frac{m\pi}{N} \right\rangle.$$

Where N is an odd positive integer and is responsible for the spacing between the states. For this encoding a complete fault tolerant gate set is provided by

$$\hat{C_{rot,N}} = \left[\hat{V_1}^{\lfloor \frac{N}{2} \rfloor} \otimes \hat{V_2}^{\lfloor \frac{M}{2} \rfloor}\right]^\dagger e^{i\pi \lfloor \frac{\hat{L_1}}{N} \rfloor \lfloor \frac{\hat{L_2}}{M} \rfloor} \left[\hat{V_1}^{\lfloor \frac{N}{2} \rfloor} \otimes \hat{V_2}^{\lfloor \frac{M}{2} \rfloor}\right],$$

$$\hat{T} = [\hat{V}^{\lfloor \frac{N}{2} \rfloor}]^\dagger e^{i\frac{\pi}{4}\lfloor \frac{\hat{L}}{N} \rfloor} e^{-i\frac{\pi}{2}\lfloor \frac{\lfloor \frac{\hat{L}}{N} \rfloor}{2} \rfloor} \hat{V}^{\lfloor \frac{N}{2} \rfloor},$$

with $\hat{S} = \hat{T}^2$ and where the Hadamard gate is implemented via a qubit teleportation scheme. For the Hadamard first a $\hat{C}_{rot}$ gate is applied to qubit as control and an ancilla in the $|+\rangle$ state. The state of the control is then measured in the X-basis. Lastly a $\hat{X}$ operator is applied to the ancilla , depending on the outcome of the measurement. These four gates form a complete gate set. This means that this encoding and these gates together provide a theoretical scheme for building a quantum computer.

5. Physical realisation: superconducting qubits

In the previous chapter a theoretical outline of a quantum computation scheme in a rotor system was outlined. In this chapter a class of physical systems, called the superconducting qubits, are discussed. Because these qubits make use of a Josephson junctions in a superconducting circuit and the description of these Josephson junction is very similar to that of the rotor, the scheme of the previous chapter could eventually be realized on such a system. The control and development of these systems however is not far developed enough to directly realize the scheme of the previous chapter, so in this chapter the focus is on some recent results in the field.

The main focus of this chapter will be on a new superconducting qubit scheme which makes use of two-Cooper-pair tunneling. This qubit design uses a Josephson junction, the basic theory of which forms the first part of this chapter, and uses ideas from the successful formula of the transmon qubit, of which a short introduction forms the second part of this chapter. The chapter is then concluded by a discussion of this two-Cooper-pair qubit.

What makes the two-Cooper-pair qubit exciting, is that it improves upon the successful formula of the transmon by having a nearly degenerate ground-state. This near degeneracy results in good predicted relaxation and dephasing times, meaning that the qubits should have longer controlled quantum effects (thus making for better possible quantum computation) [10]. A full discussion of these two-Cooper-pair qubits goes beyond the scope of this project, such that we mainly focus here on the Hamiltonian and deriving some properties of the eigenstates.

5.1 The Josephson junction

In the simplest terms a Josephson junction is explained as a very small piece of insulating metal between the superconducting wires in a circuit. Since the electrons classically can not move through the insulating piece of metal, they have to tunnel, describing the quantum mechanical behavior of the system. A picture and schematic representation of the junction is presented below. This section is based on [28].

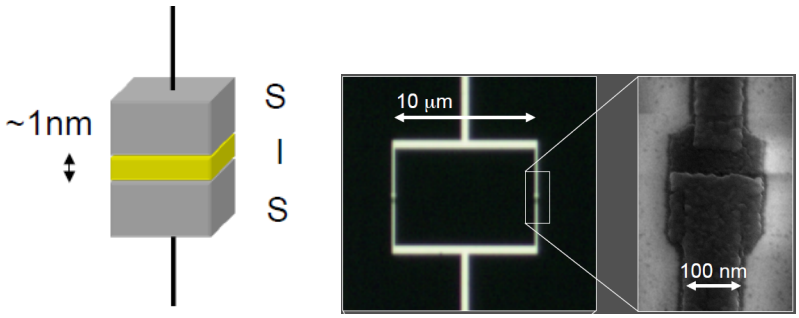

Figure 5.1: (a) a schematic representation of a Josephson junction. The grey metal is a superconductor and the yellow metal is an insulator, thus this demonstrates that the Josephson junction is a superconductor-insulator-superconductor tunnel junction. (b) A microscopic picture of a Josephson junction. The junction is here created with an Aluminium-Aluminiumoxide-Aluminium stack.

As noted above, the Josephson junction divides two superconducting wires. These superconducting wires show a quantum mechanical behaviour which can be described using the number of Cooper pairs and the phase. The derivation of this fact is lengthy and irrelevant for the rest of the section, thus we refer to [28]. The main point is that the state can be described as

$$|\Psi_{superconductor}\rangle = \sum_{n=0}^{\infty} |\lambda_n| e^{i\phi\frac{n}{2}} |n\rangle \tag{5.1}$$

Where $|n\rangle$ denotes the number of electrons in the wire and ϕ refers to the phase associated of the superconductor.

Now in order to describe the effect of the junction the difference between the two superconducting states is used. To describe the effect of the junction on the number of electrons the difference in number of Cooper pairs (as result of tunneling) is introduced, this is defined by

$$|m\rangle = |N_r - m\rangle |N_l + m\rangle, \tag{5.2}$$

where N_r is the number of Cooper pairs one side of the junction. here called the right side, and N_l the number on the other, here the left. Important to note is that while the number of Cooper pair states is always a positive integers, the difference in number states can also be negative (by there being more Cooper pair tunneled to the right), such that $m \in \mathbb{Z}$. Secondly to describe the effect of the junction on the phases of the wires the difference in the phase of the two states is also introduced, this is defined as

$$\phi = \Delta\phi = \phi_{wire,1} - \phi_{wire,2}. \tag{5.3}$$

Because only the phase difference is an important parameter, this is commonly referred to as the phase of whole junction (although it is actually a phase difference between the two sides of the junction).

These parameters behave analogous to a rotor system. In this analogy the difference in the number of electrons $|m\rangle$ plays the role the angular momentum states $|l\rangle$ and the phase ϕ plays the role of the angular position θ. The Hilbert spaces of $|m\rangle \in l^2(\mathbb{Z})$ and $|\phi\rangle \in L^2([0, 2\pi])$, as in the rotor case, are related by the discrete Fourier transform. (For more on these operators see chapter 1.)

Now to calculate the effect of the junction on the Hamiltonian of the system, the amount of energy stored in the junction is of interest. The amount of current that will flow through the junction is given by

$$I_{junc} = I_c sin(\phi), \tag{5.4}$$

where I_c is the maximal current the junction can support. The Voltage bias of the junction is given by

$$V_{junc} = \frac{\hbar}{2e}\frac{d\phi}{dt}. \tag{5.5}$$

Combining these results the energy stored in the junction can calculated by

$$H_j = \int I_{junc} V_{junc} dt = \int I_c sin(\phi) \frac{\hbar}{2e}\frac{d\phi}{dt} dt = \frac{\hbar I_c}{2e}\int sin(\phi) d\phi = const. - E_j cos(\phi), \tag{5.6}$$

with the Josephson energy $E_j = \frac{\hbar I_c}{2e}$.

To summarize, the Josephson junction is described using the difference in Cooper pairs $|m\rangle$ and the phase (difference) ϕ, which function analogously to the angular momentum and angular position of a rotor. The energy stored in the Junction is given by $-E_j cos(\phi)$, with $E_j = \frac{\hbar I_c}{2e}$.

5.2 The transmon qubit

As noted in the introduction, the transmon qubit design is one of the most successful superconducting qubits. In this section the encoding and idea behind a transmon qubit is only shortly reviewed, since the main focus of the chapter is on the two-Cooper-pair qubit. For a full discussion of the transmon qubit see [29]. This section, being somewhat more elementary, is based on [30] and [28].

The building of the transmon started as the idea of encoding a qubit in an harmonic oscillator. These qubits are however not encoded like in section 3.2, for which the level of control is not yet high enough, but are encoded in a simpler fashion by taking the two lowest energy levels of the oscillator. By only using these two states, this subsystem behaves like a qubit system.

The attractiveness of this idea comes from how easy the system is to obtain. A simple LC-circuit (see the figure below) behaves like an harmonic oscillator and the gap between energy levels of the system can be very easily engineered. Since $E_n = (\frac{1}{2} + n)\hbar\omega_r$ with $\omega_r = \frac{1}{\sqrt{LC}}$, any energy spacing can be obtained. The problem with building a qubit in an harmonic oscillator is that the energy difference between all the energy levels is the same. As a consequence the process of changing the state from $|0\rangle$ to $|1\rangle$ costs the same as $|1\rangle$ to $|2\rangle$. This forms a problem, because any external energy supply used to operate the qubit operations (for instance microwave radiation) can move both $|0\rangle \rightarrow |1\rangle$ and $|1\rangle \rightarrow |2\rangle$ at the same time. This means that the state leaks out of the required two lowest levels, which leads to errors in the computation.

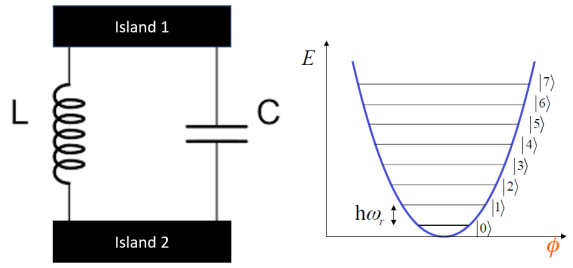

Figure 5.2: (a) a schematic representation of a LC-circuit and (b) the equal spaced energy states of the harmonic oscillator.

The innovation of the transmon qubit is to get around this problem by introducing an anharmonious element in the oscillator by replacing the inductance by a Josephson junction (see the figure below). This anharmonious element causes the states to be spaced unevenly, which makes it possible to find a regime where the states have a good coherence time and do not leak too easily into the states of $|2\rangle$ and up (but leakage can still happen).

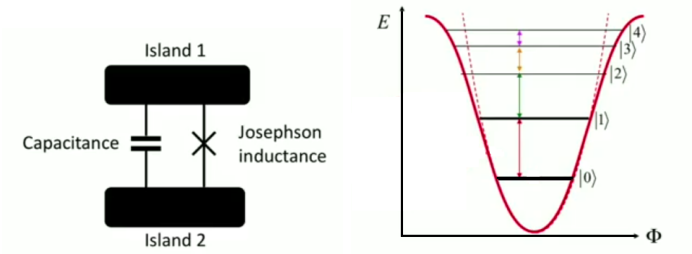

Figure 5.3: (a) a simplified schematic representation of a transmon circuit and (b) the unequal spaced energy states introduced by the Josephson junction.

The Hamiltonian of this system is given by

$$\hat{H}_{transmon} = 4E_c(\hat{n} - n_g\hat{I})^2 - E_j cos(\hat{\phi}). \tag{5.7}$$

Here $\hat{n}$ is related the charge state operator (by $\hat{Q} = 2e\hat{n}$) and it acts on the Cooper pair difference of the Josephson junction as $\hat{n}\,|m\rangle = m\,|m\rangle$. n_g is the gate charge offset in the system and as previously discussed $E_j\hat{cos}(\phi)$ is the energy in the junction.

Now to see the power of the transmon the effect of the energy ratio $\frac{E_c}{E_j}$ is crucial. The effect of this ratio is twofold. On increasing the ratio on the one hand the effect of the charge noise in the form of n_g is decreased, which fluctuates as it is induced by some external Voltage V_g, but on the other hand the level of anharmonicity of the system decreases (thus increasing leakage in the

system). But since the first effect decreases exponentially and the second only algebraically, there exist an optimal regime for the ratio. In this regime, the qubit is quite well protected from charge noise, having a decoherence time roughly between $10\mu s - 100\mu s$ for realistic parameters [28], and the states are divided well enough to avoid (too much) leakage. This central property makes the transmon a very successful qubit encoding.

5.3 Two-Cooper-pair qubit

The new two-Cooper-pair qubit takes many of its ideas from the original transmon (especially the way in which it avoids charge noise is very similar) and improves upon the formula by having the two lowest energy states be nearly degenerate. This improvement should allow the circuit to have even longer coherence times, since the phase-difference obtained over time, given $\frac{(E_1-E_0)t}{\hbar}$ (remember that for any stationary state $\Psi_n(t) = \Psi_n(0)e^{-i\frac{E_n t}{\hbar}}$), is even smaller. But since the scheme of this qubit is so recently designed, there are no experimental results as of the moment of writing.

For these qubits first a short overview is presented of the circuit used to create the two-Cooper-pair tunneling. After this an in depth discussion of the Hamiltonian describing the system is presented. The circuit and Hamiltonian are from [10].

The circuit

The circuit of the two-Cooper-pair qubit makes use of an inductive element and a capacitance in parallel as in the LC and in the transmon circuits. Here the inductive element consists of two Josephson junctions placed in parallel, both placed in the middle of two superinductances (see the figure below). This parallel composition only allows for the tunneling of two Cooper-pair electrons at the same time.

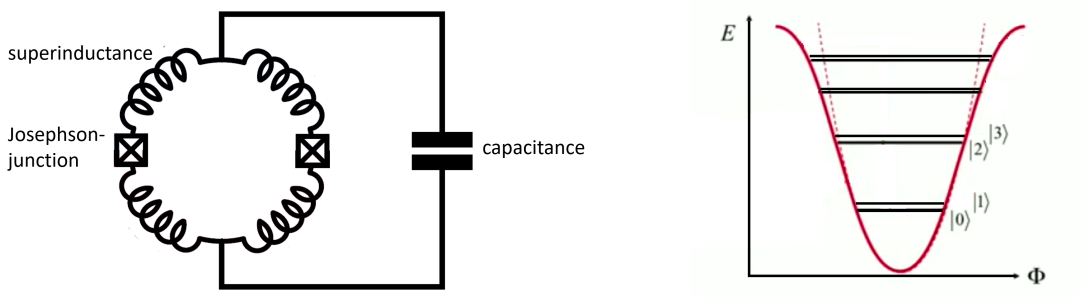

Figure 5.4: (a) a simplified schematic representation of a two-Cooper-pair tunneling circuit and (b) the unequal, nearly degenerate, spaced energy states introduced by the circuit. The energies in (b) are not representative of the exact scale, but provide some idea of the energy spectrum.

The Hamiltonian

The Hamiltonian of the circuit is approximated by [10]

$$\hat{H} = 4E_c(\hat{n} - n_g\hat{I})^2 - E_j cos(2\hat{\phi}), \tag{5.8}$$

where the operators mean the same as in equation 5.7. The only difference between the two Hamiltonians is that the $cos(\phi)$ from the transmon is now replaced by a $cos(2\phi)$.

First the question of where the $cos(2\phi)$ element comes from. The $cos(2\phi)$ element is a direct consequence of only letting two Cooper pairs tunnel at same time. This can be seen as follows. As noted before, the energy of the Josephson junction is given by $-E_j cos(\hat{\phi})$. Now by Euler's formula note that $cos(\hat{\phi}) = \frac{1}{2}(e^{i\hat{\phi}} + e^{-i\hat{\phi}}) = \frac{1}{2}(\hat{V} + \hat{V}^\dagger)$ (see chapter 1), thus letting a Cooper-pair tunnel is represented as a right and a left shift in the difference of electrons. By letting only two Cooper-pairs tunnel the result is twice the shift, this gives $\frac{1}{2}(\hat{V}^2 + \hat{V}^{\dagger 2}) = \frac{1}{2}(e^{i2\hat{\phi}} + e^{-i2\hat{\phi}}) = cos(2\hat{\phi})$, which shows how the $cos(2\phi)$ is obtained.

Using the representation $\frac{1}{2}(\hat{V}^2 + \hat{V}^{\dagger 2})$ of the two-Cooper-pair element and the commutation relation from chapter 1 of

$$\hat{V}^k e^{i\alpha\hat{n}} = e^{ik\alpha} e^{i\alpha\hat{n}} \hat{V}^k, \tag{5.9}$$

the following commutation can be derived (since $e^{i2\pi} = 1$)

$$e^{i\pi\hat{n}} \hat{H} e^{-i\pi\hat{n}} = \hat{H}. \tag{5.10}$$

From this commutation it can be concluded that $e^{i\hat{\pi}L}$ and $\hat{H}$ share eigenfunctions. This means that the eigenfunctions of $\hat{H}$ are given by either even or odd number of Cooper states. These eigenstates will have nearly the same energy and be orthogonal for each energy level.

To further study the eigenfunctions, the Hamiltonian is represented on the phase space of $L^2([0, 2\pi])$. After using separation of variables the time-independent form of the Schrödinger equation is given by

$$4E_c \left(-\frac{\partial^2\Psi(\phi)}{\partial\phi^2} - 2n_g i\frac{\partial\Psi(\phi)}{\partial\phi} + n_g^2\right) - E_j cos(2\phi)\Psi(\phi) = E\Psi(\phi), \tag{5.11}$$

which is a differential equation with periodic boundary conditions $\Psi(\phi) = \Psi(\phi + 2\pi)$. Now using the substitution of $g(\phi) = e^{i\phi n_g}\Psi(\phi)$, the differential equation reduces to

$$\frac{\partial^2 g(\phi)}{\partial\phi^2} + \left(\frac{E}{4E_c} - \frac{E_j}{4E_c} cos(2\phi)\right) g(\phi) = 0. \tag{5.12}$$

This differential equation is known as the Mathieu equation. From the substitution above, it can be concluded that the solutions of the Mathieu equation will provide the eigenfunctions and eigenvalues of the original Hamiltonian.

First the eigenvalues are discussed. In order to find a physical solution, the solution of the state has to be bounded (to be normalizable), or "stable". A stability chart of the Mathieu functions is given in the figure below.

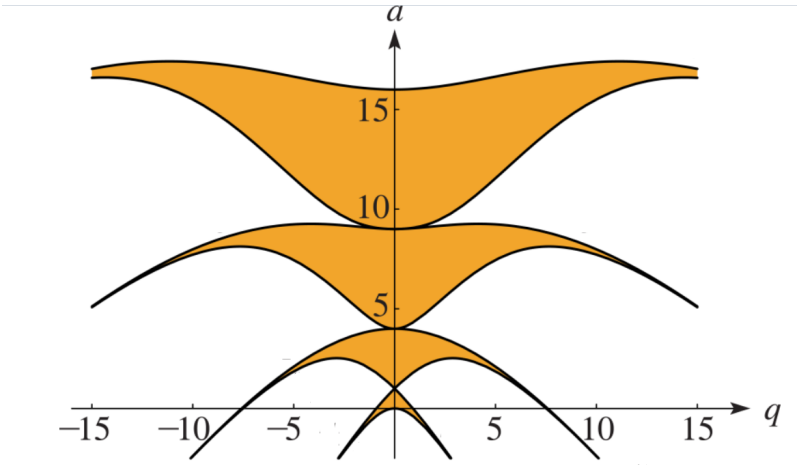

Figure 5.5: The stability chart of the Mathieu function for different values of $a = \frac{E}{4E_c}$ and $q = \frac{E_j}{8E_c}$. The region with stable solutions is denoted by the orange surface in the plot. The orange region depicts four bands of stable solutions here. The figure is from [31].

Any eigenvalue of the original equation has to be in the orange region. The solutions are even further fixed by the boundary conditions for $g(\phi)$, obtained by the original $\Psi(\phi) = \Psi(\phi + 2\pi)$, given by

$$g(\phi) = e^{-i2n_g\pi} g(\phi + 2\pi). \tag{5.13}$$

From this boundary condition it follows that there are only two energy value per band (more on this later). With this information an upper bound to the difference between the energy level in

a band can be obtained, since the energy difference will be smaller than the height of the energy band of the bands in figure 5.5. Hereby the following result is obtained for large $\frac{E_j}{E_c}$ (from [31] section 28.8)

$$\Delta E \leqslant \frac{2^{4m+5}}{m!}\sqrt{\frac{2}{\pi}}\left(\frac{E_j}{8E_c}\right)^{\frac{2m+3}{4}} e^{-\sqrt{\frac{2E_j}{E_c}}}\left(1-\frac{(6m^2+14m+7)\sqrt{8E_j}}{32\sqrt{E_c}}+O\left(\frac{E_c}{E_j}\right)\right). \tag{5.14}$$

Where $m \in \mathbb{N}_0$ denotes the number of the energy band. This shows, that the two lowest energy levels, by taking m = 0, for large $\frac{E_j}{E_c}$, are nearly degenerate as claimed before.

Now for the eigenfunctions associated to these energies, things become a lot more tricky. The Mathieu equation has no solutions in a closed form, meaning some expression of the form $f(x) = ...$ does not exist. Still the equation has been studied thoroughly (see [32] and [31]) and therefore a lot of properties of the solution are known. (A nice discussion of the Mathieu functions for this Hamiltonian is also given in [33], though it is unpublished work.) Here some of these properties, those relevant to this Hamiltonian, are discussed.

First it is noted that equation 5.12 is periodic in ϕ, with period π. Now by Floquet's or Bloch's theorem any solution has to be of the form

$$g(\phi+\pi) = e^{i\pi\nu}g(\phi), \tag{5.15}$$

with $\nu \in \mathbb{R}$ the characteristic exponent (Floquet) or the wave vector (Bloch). By equation 5.13 it can be concluded that ν can only take the form of

$$\nu = -n_g + k, k \in \mathbb{Z} \tag{5.16}$$

This result has some important consequences. First two general properties of the solutions. The result of 5.16 implies that for any charge offset n_g the solution $\Psi_m(\phi)$ is either periodic or anti-periodic in ϕ with period π, meaning

$$\Psi_m(\phi+\pi) = (-1)^m\Psi_m(\phi), \tag{5.17}$$

where $m \in \mathbb{N}$ labels the eigenfunctions.

A second general property is the already mentioned two solutions per energy band. While a formal proof is given in [33], this can easiest be understood graphically in the figure below.

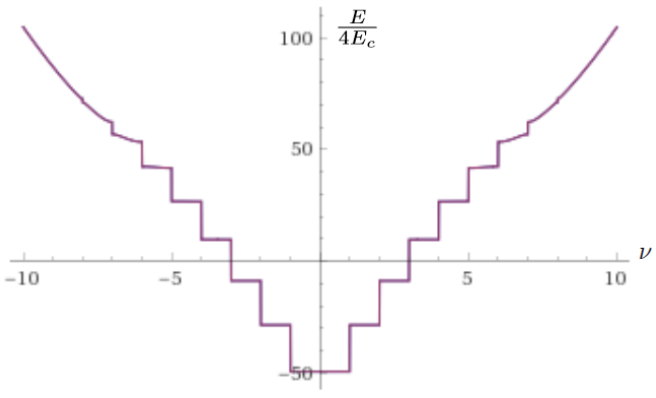

Figure 5.6: The eigenvalues $\frac{E}{4E_c}$ values on the y-axis versus the Floquet exponent on the x-axis for the Hamiltonian of 5.11 at $\frac{E_j}{8E_c} = 30$. This graph depicts relation between the eigenvalues and the Floquet exponent for a general Mathieu equation, thus all values for the Floquet exponent are possible. In the case of the Hamiltonian from equation 5.11 the possible Floquet exponents are further fixed by equation 5.16.

When fixing a value of n_g, it can easily be seen that a displacement of $k \in \mathbb{Z}$ places the Floquet exponent each time in a new band. But more importantly the degenerate solutions are for each

n_g separated by a an odd number of displacements (meaning $m = 2k + 1$ for some $k \in \mathbb{Z}$) and that these two solutions exhaust all solutions in the energy band [33]. This property is crucial for proving some error resistant characteristics of the system.

The second consequence from result 5.16 lies in the form of the degenerate eigenfunctions. The eigenfunctions of the Mathieu equation are called the Mathieu functions and are for $\nu \in \mathbb{R}$ denoted by $me_\nu^{(n)}(\phi)$, where $n \in \mathbb{N}$ labels associated the energy bands. Using the properties of the Mathieu functions it is proven here that the eigenfunctions in the same energy band are of the same form on $[0, \pi]$, but differ only in their (anti-)periodicity.

Following the reasoning used in [32], we use an expansion of the Mathieu function for a general Mathieu equation. Let $t = e^{i\pi\nu}$, where the choice of ν is only restricted by having to imply a stable solution (since we are talking here about the Mathieu equation in its general form). The function $v_n(z,t) = me_\nu^{(n)}(z)$ is an analytic function on the ring $R : 1 - \delta \leqslant |t| \leqslant 1 + \delta$ with $\delta \in \mathbb{R}$ small (such that the solutions exists on the whole ring). Thus $v_n(z,t)$ has a Laurent decomposition of

$$v_n(z,t) = \sum_{m\in\mathbb{Z}} a_m^{(n)}(z)t^m \tag{5.18}$$

which leads by taking using the Cauchy integral theorem on

$$a_m^{(n)}(z) = \frac{1}{2\pi i} \oint \frac{v_n(z,\tau)}{\tau^m + 1} d\tau \tag{5.19}$$

to the decomposition of $me_\nu^n(z)$ of

$$me_\nu^{(n)}(z) = \sum_{m\in\mathbb{Z}} a_m^{(n)}(z)e^{im\pi\nu}. \tag{5.20}$$

Since $me_\nu^{(n)}(z)$ has to satisfy the condition of 5.15, this decomposition can be simplified to

$$me_\nu^{(n)}(z) = \sum_{m\in\mathbb{Z}} a_0^{(n)}(z - m\pi)e^{im\pi\nu}. \tag{5.21}$$

(see also [32] sect. 2.34.). This decomposition holds for any Mathieu equation [32].

Using this decomposition we will prove that, for the Hamiltonian of equation 5.11, one solution in an energy band is periodic if and only if the other solution anti-periodic. Here we use that for this Hamiltonian it holds that (as was noted above) given that the Floquet exponent ν_1 is a solution to the original equation of 5.12, the other solution in the same energy band can be obtained by filling in $\nu_1 + l$ for some odd l. Also it was remarked that these two solutions form all the solutions in the energy band. Now suppose that $me_{\nu_1}^{(n)}(z)$ is a solution of equation 5.12. Filling the Floquet exponent $\nu_2 = \nu_1 + l$ of the other solution in the decomposition of equation 5.21 it is obtained that the degenerate solutions are of the form

$$me_{\nu_1}^{(n)}(z) = \sum_{m\in\mathbb{Z}} a_0^{(n)}(z - m\pi)e^{im\pi\nu_1} \text{ and} \tag{5.22a}$$

$$\begin{aligned} me_{\nu_2}^{(n)}(z) = me_{\nu_1+l}^{(n)}(z) &= \sum_{m\in\mathbb{Z}} a_0^{(n)}(z - m\pi)e^{im\pi(\nu_1+l)}, \\ &= \sum_{m\in\mathbb{Z}} a_0^{(n)}(z - m\pi)(e^{i\pi})^{ml}e^{im\pi\nu_1}, \\ &= \sum_{m\in\mathbb{Z}} a_0^{(n)}(z - m\pi)(-1)^m e^{im\pi\nu_1}, \end{aligned} \tag{5.22b}$$

using in the second step that ml is odd if and only if m is odd, since l has to be odd. From these decompositions of the two solutions we conclude that the solutions in a given energy band are the same on $[0, \pi]$, with one being periodic over π and the other anti-periodic over π. Since these solutions exhaust all possible solutions in a given energy band, the proof is complete.

Since for degenerate eigenfunctions the solutions only differ in their (anti-)periodicity, it is concluded that their orthogonality is stable under a small shift. This means that if Ψ_0, Ψ_1 are the

normalized solutions in the same energy band that for a small shift $e^{i\alpha\hat{L}}$ with $\alpha \in \mathbb{R}$ small, it holds that $\langle\Psi_0| e^{i\alpha\hat{L}} |\Psi_1\rangle \approx 0$. Secondly the superpositions of $\Psi_\pm = \frac{1}{\sqrt{2}}(\Psi_0 \pm \Psi_1)$ have zero support on $[\pi, 2\pi]$ for Ψ_+ and $[0, \pi]$ for Ψ_-. For the lowest energy state the states will then be localised near $0, \pi$ respectively, since the potential energy is lowest at $0, \pi$ and for the lowest energy there is little tunneling. For this reason also their orthogonality is stable under small shifts, meaning $\langle\Psi_+| e^{i\alpha\hat{L}} |\Psi_-\rangle \approx 0$. This shows some of the error resistant qualities of the system.

Thus from the analysis of the Hamilton 5.11 the following results can be concluded. The two lowest energy states are nearly degenerate, where their degeneracy scales with a dominant term of $e^{-\sqrt{\frac{2E_j}{E_c}}}$ for large $\frac{E_j}{E_c}$. This degeneracy means that the lowest energy states will only obtain a very small phase difference over time, which is an important property for long coherence times. Secondly the solutions in the same energy band have the same form on $(0, \pi)$ and differ on $(\pi, 2\pi)$ only by their (anti-)periodicity. This means that the superpositions $\Psi_\pm = \frac{1}{\sqrt{2}}(\Psi_0 \pm \Psi_1)$ are localized close to $0, \pi$ respectively. This means that the two Cooper pair qubit already shows some promise for realizing the zero spacing encoding from the previous chapter (see 4.1) and since it inherits the same techniques as the transmon to protect the qubit from charge noises (which corresponds to angular momentum shifts in the rotor picture) this zero spacing is a justified assumption here. Thus, while a full realization of the scheme from chapter 4 still are far away, the encoding for zero angular momentum spacing seems realizable.

Conclusion

As said in the introduction, the goal of this report was to study error correcting encodings of qubits in a rotor space. The rotor space was described using the angular momentum $\hat{L}$ and the angular position $\hat{\Theta}$, where the expressions of the states in the different bases were related by the discrete Fourier transform. The possible errors on the states in the rotor space were given by shifts, $\hat{V}$ the angular momentum shift and $e^{i\alpha\hat{L}}$ the angular position shift. To protect the encoding a shift resistant encoding was used. Here small shift in the code can be detected by a stabilizing measurement and then corrected. Since large errors are seen as the accumulation of small errors, the encoding should be error resistant.

The ideal shift resistant encoding of the rotor space was given by

$$|\bar{0}\rangle = \sum_{l\in\mathbb{Z}} |2Nl\rangle = \sum_{m=0}^{2N-1} \left|\theta = \frac{m\pi}{N}\right\rangle,$$

$$|\bar{1}\rangle = \sum_{l\in\mathbb{Z}} |2Nl+N\rangle = \sum_{m=0}^{2N-1} (-1)^m \left|\theta = \frac{m\pi}{N}\right\rangle.$$

Where the spacing between the states is given by an odd positive integer N. For a zero spacing $N = 1$ is used. For this encoding a complete fault tolerant gate set was provided by

$$\hat{C_{rot,N}} = \left[\hat{V_1}^{\lfloor\frac{N}{2}\rfloor} \otimes \hat{V_2}^{\lfloor\frac{M}{2}\rfloor}\right]^\dagger e^{i\pi\lfloor\frac{\hat{L_1}}{N}\rfloor\lfloor\frac{L_2}{M}\rfloor}\left[\hat{V_1}^{\lfloor\frac{N}{2}\rfloor} \otimes \hat{V_2}^{\lfloor\frac{M}{2}\rfloor}\right],$$

$$\hat{T} = [\hat{V}^{\lfloor\frac{N}{2}\rfloor}]^\dagger e^{i\frac{\pi}{4}\hat{\lfloor\frac{L}{N}\rfloor}} e^{-i\frac{\pi}{2}\hat{\lfloor\frac{\lfloor\frac{L}{N}\rfloor}{2}\rfloor}} \hat{V}^{\lfloor\frac{N}{2}\rfloor},$$

with $\hat{S} = \hat{T}^2$ and where the Hadamard gate is implemented via a bit teleportation bit scheme. For the Hadamard first a $\hat{C_{rot}}$ gate is applied, then a measurement in the X-basis on the original and lastly the X operator is applied controlled by the measurement. These four gates formed a complete gate set. This means that this encoding and these gates together provide a theoretical scheme for building a quantum computer.

While the construction of an actual quantum computer following the scheme from above is still far away, because of the high level of state preparation and the hard to realize floored angular momentum operator (given by $\lfloor\frac{\hat{L}}{k}\rfloor$ with $k \in \mathbb{Z}$). A recent superconducting qubit scheme shows some promise in parts of the realization. This two-Cooper-pair qubit allows only pairs of Cooper pairs to tunnel through a Josephson junction. The resulting state is described by the difference in Cooper pairs between the sides of the junction, which was described using the same Hilbert space as angular momentum, and the phase across the junction, which was analogue to the angular position state. In this two-Cooper pair scheme, the two lowest energy states are nearly degenerate, are similar on $(0, \pi)$ and differ on $(\pi, 2\pi)$ only by their (anti-)periodicity. Of the two states one consisted of only an even difference in Cooper pairs and the other of only an odd difference, which corresponds roughly to the $|0\rangle, |1\rangle$ in the zero spacing encoding from above. Using these lowest energy states a superpositions localized near 0 and π can be constructed, which corresponds to the $|\pm\rangle (= \frac{1}{\sqrt{2}}(|0\rangle \pm |1\rangle))$ in the zero spacing scheme from the encoding above. This means that, while the implementation of the fault tolerant gate set seems very far away, the two-cooper-pair qubit is able to replicate the zero space encoding presented above.

Acknowledgments

Foremost I would like to thank Prof. Dr. Van Neerven and Prof. Dr. Terhal for the opportunity to write a thesis under their supervision. From their guidance, feedback and discussions I have learned so much. Secondly, I would like to thank Jonathan Conrad, Christophe Vuillot and Daniel Weigand from the Terhal group for their willingness to help when I was stuck, their openness and the enlightening discussions. Especially Jonathan for his help and feedback with writing.

Bibliography

[1] *Roadmap Qutech*. https://qutech.nl/roadmaps/, visited 2019-07-02.

[2] *Quantum Computing at IBM* . https://www.research.ibm.com/ibm-q/learn/what-is-ibm-q/, visited 2019-07-02.

[3] *Empowering the quantum revolution*. https://www.microsoft.com/en-us/quantum/, visited 2019-07-02.

[4] *Quantum* . https://ai.google/research/teams/applied-science/quantum-ai/, visited 2019-08-26.

[5] John Preskill. Quantum computing in the nisq era and beyond. *Quantum*, 2:79, 2018.

[6] Peter W Shor. Polynomial-time algorithms for prime factorization and discrete logarithms on a quantum computer. *SIAM review*, 41(2):303–332, 1999.

[7] Aram W Harrow and Ashley Montanaro. Quantum computational supremacy. *Nature*, 549(7671):203, 2017.

[8] Iulia Buluta and Franco Nori. Quantum simulators. *Science*, 326(5949):108–111, 2009.

[9] P. Raynal, A. Kalev, J. Suzuki, and B. Englert. Encoding many qubits in a rotor. In *AIP Conference Proceedings*, volume 1469, pages 63–81. AIP, 2012.

[10] Kou A. Xiao X. Vool U. Smith, W. and M. Devoret. Superconducting circuit protected by two-cooper-pair tunneling. *arXiv preprint arXiv:1905.01206*, 2019.

[11] P Carruthers and M. Nieto. Phase and angle variables in quantum mechanics. *Reviews of Modern Physics*, 40(2):411, 1968.

[12] P. Busch, M. Grabowski, and P. Lahti. *Operational quantum physics*, volume 31. Springer Science & Business Media, 1997.

[13] J. van Neerven. An introduction to functional analysis, 2018.

[14] L. Susskind and J. Glogower. Quantum mechanical phase and time operator. *Physics Physique Fizika*, 1(1):49, 1964.

[15] A. Grimsmo, J. Combes, and B. Baragiola. Quantum computing with rotation-symmetric bosonic codes. *arXiv preprint arXiv:1901.08071*, 2019.

[16] D.J. Griffiths. *Introduction to Quantum Mechanics*. Pearson international edition. Pearson Prentice Hall, 2005.

[17] M. Veraar. Measure and integration, 2017.

[18] B. Hall. *Quantum theory for mathematicians*, volume 267. Springer, 2013.

[19] J. Garrison and J. Wong. Canonically conjugate pairs, uncertainty relations, and phase operators. *Journal of Mathematical Physics*, 11(8):2242–2249, 1970.

[20] D. Gijswijt. Algebra 1, 2019.

[21] M. Ozols. Clifford group. *Essays at University of Waterloo, Spring*, 2008.

[22] Bruce E Kane. A silicon-based nuclear spin quantum computer. *nature*, 393(6681):133, 1998.

[23] Resch K. Rudolph T. Schenck E. Weinfurter H. Vedral V. Aspelmeyer M. Walther, P. and A. Zeilinger. Experimental one-way quantum computing. *Nature*, 434(7030):169, 2005.

[24] D Gottesman, A Kitaev, and J Preskill. Encoding a qubit in an oscillator. *Physical Review A*, 64(1):012310, 2001.

[25] E. Knill and Laflamme. Theory of quantum error-correcting codes. *Physical Review A*, 55(2):900, 1997.

[26] B Terhal. Quantum error correction for quantum memories. *Reviews of Modern Physics*, 87(2):307, 2015.

[27] M. A. Nielsen and I. Chuang. *Quantum computation and quantum information*. AAPT, 2002.

[28] F. Pedrocchi. Introduction to transmon qubits: Model and simple operations, 2016.

[29] Terri M. Gambetta J. Houck A . Schuster D. Majer J. Blais A. Devoret M. Girvin S. Koch, J. and R. Schoelkopf. Charge-insensitive qubit design derived from the cooper pair box. *Physical Review A*, 76(4):042319, 2007.

[30] L. DiCarlo. The transmon qubit | qutech academy. `https://www.youtube.com/watch?v=cb_f9KpYipk&list=PL5jmbd6SJYnPiYlM6pHAm2M3FL40D9otZ&index=15&t=0s`, 2018.

[31] *NIST Digital Library of Mathematical Functions*. http://dlmf.nist.gov/, Release 1.0.23 of 2019-06-15. F. W. J. Olver, A. B. Olde Daalhuis, D. W. Lozier, B. I. Schneider, R. F. Boisvert, C. W. Clark, B. R. Miller and B. V. Saunders, eds.

[32] Josef Meixner and Friedrich Wilhelm Schäfke. *Mathieusche Funktionen und Sphäroidfunktionen: mit Anwendungen auf physikalische und technische Probleme*, volume 71. Springer-Verlag, 2013.

[33] D. Weigand and B. Terhal. Rotor qubit *(unpublished)*, 2018.